6.
DUAL-BAND ANTENNA FOR ULTRA AND SUPER HIGH FREQUENCY RFID TAGS

6.1. Introduction

In the previous chapter (chapter five), the novel single sided dual antenna structure for UHF RFID tag which works at 915 MHz is presented. It is suitable for both metallic and non-metallic surfaces. However, RFID systems work on four different bands, i.e., (low-frequency (LF) (125-134 kHz), high-frequency (HF) (13.56 MHz), UHF (860-960 MHz), and super high frequency (SHF) (2450 MHz or 5800 MHz). Therefore, it is desirable to design dual antenna structure capable of operating in multiple RFID frequency bands.

Various dual band tag antennas have been reported in which single antenna structure is used for both receiving and backscattering modes. The majority of which combine the HF (13.56 MHz) and UHF (915 MHz) bands [Ma *et al.* (2012), Iliev *et al*. (2010), Mayer and Scholtz (2008)] or UHF (866 MHz) and UHF (915 MHZ) bands [Du *et al.* (2013), Kim and Yeo (2012), Paredes *et al.* (2011), Huang *et al.* (2010), Paredes *et al*. (2010)], or UHF and SHF (2450 MHz) bands [Jeon *et al.* (2006), Grilo *et al*.(2012), Kimouche *et al.* (2009), Kimouche and Zemmour (2011), Wu *et al*. (2011)]. To the best of the knowledge, none of the papers are available with dual antenna structure on most promising UHF and SHF bands.

In this chapter, a single sided dual-band antenna for RFID tag is presented to cover 915 MHz (UHF) and 2450 MHz (SHF) frequencies. Due to single-sided antenna structure with the complete ground plane, the proposed tag antenna can also be used with metallic objects without performance degradation opposite to the conventional tag antennas. The proposed tag antenna is a dual antenna structure at UHF band and conventional single antenna at SHF. For 915 MHz application, proposed antenna consists of two independent antennas one for receiving (Antenna-I) and the other for backscattering (Antenna-II) which enhances the read range [Chen *et al.* (2011)a]. Whereas for 2450 MHz

application, proposed antenna behaves like a conventional single antenna in which receiving and backscattering operation are performed by the same antenna (Antenna-I). Due to which Antenna-II is not utilized at 2450 MHz. The Antenna-I is made up with an F-shaped slot and an inverted L-shaped slot loaded rectangular patch antenna whereas Antenna-II made up with meandered line structure. The dual-band behaviour of the Antenna-I is achieved by proper optimization of the F-shaped and an inverted L-shaped slots. The performance of proposed antenna is evaluated in terms of RCS, gain, and read range. The antenna design concepts along with simulated and measured results are discussed in the following sections. All the simulations were performed using finite element method (FEM) based Ansys's high frequency structure simulator (HFSS) [HFSS ver. 14.0].

6.2. Antenna Configuration

The geometry and fabricated prototype of the proposed dual-band dual antenna structure for UHF and conventional single antenna for SHF RFID tag is shown in Figures 6.1(a) and 6.1(b), respectively. The proposed dual antenna structure works with a tag IC having three terminals instead of two terminals in conventional tag ICs for single antenna structure. The three terminals of tag IC for dual antenna structure are denoted as RF1, RF2, and common ground. RF1 and RF2 are connected to the signal terminals of the receiving antenna and the backscattering antenna, respectively. The ground terminal is connected to the other terminals of both the antennas.

The antenna is fabricated on low cost FR4 substrate having dielectric constant (ε_r) 4.4, loss tangent ($tan\ \delta$=0.018), and thickness 1.6 mm. The proposed antenna is designed for Impinj Monza Gen2 tag chip with input impedance of 33-j112Ω at 915 MHz [Monza4 Tag] and 50Ω at 2450 MHz. Initially, Antenna-I consists of two back to back inverted L-shaped slits loaded patch antenna for dual-band operation. After, rigorous optimization of slits and antenna shape parameters, UHF and SHF bands resonate at 915 and 2480 MHz, respectively. To tune the SHF band at 2450 MHz, an additional slit is added to the right hand side

of the inverted L-shaped slit to make the F-shaped slit. Due to which electrical length of patch increases and resonance frequency decreases from 2480 MHz to 2450 MHz. Finally, the Antenna-I consists of an F-shaped, and an inverted L-shaped slits loaded rectangular patch is evolved. Antenna-II consists of meandered line structure. Both the antennas are connected to the tag chip through a cylindrical via. The actual overall size of the antenna is 70 mm × 80 mm.

The optimized value of the shape parameters of the proposed antenna are shown in Table 6.1. The Antenna-I is designed in such a way that the input impedance of receiving antenna at 915 MHz and 2450 MHz is complex conjugate of the tag chip so that maximum power is transferred to the antenna. These two design frequencies are achieved by tuning the length and width of slot parameters of Antenna-I.

Antenna-II is utilized for backscattering of 915 MHz to achieve maximum impedance difference between open and short circuit during operations of tag, which helps to maximize the read range.

To design of the antenna, first, we used a rectangular patch and two vertical line slots (Ly2) along with shorting pin which is connected to ground, as shown in Figure 6.2. The impedance of the antenna at 915 MHz and power reflection coefficient at 2.45 GHz is presented in Figure 6.2 (a) and Figure 6.2(b). In next step, we added two narrow horizontal slots (Lx1) at the end of vertical slots as shown in Figure 6.3. The impedance of the antenna at 915MHz and power reflection coefficient at 2.45 GHz is presented in Figure 6.3(a) and Figure 6.3(c). And finally to adjust the higher frequency the small slot has been added (Lx3) Figure 6.4. The impedance of the antenna at 915MHz and power reflection coefficient at 2.45 GHz is presented in Figure 6.4(a) and Figure 6.4(b).

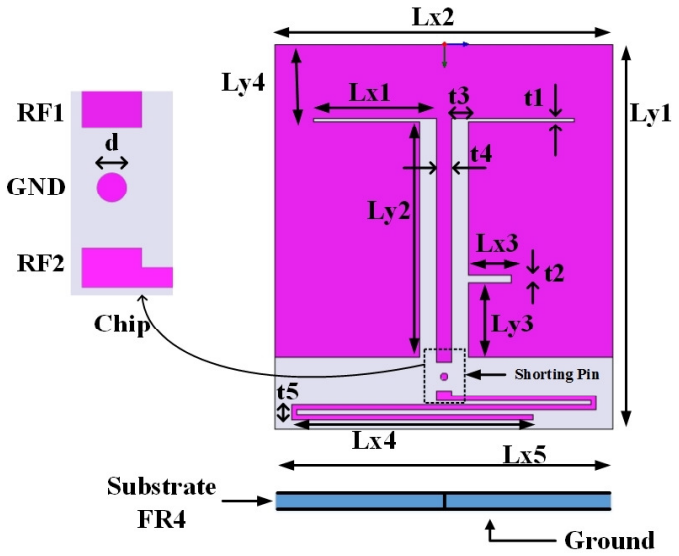

(a)

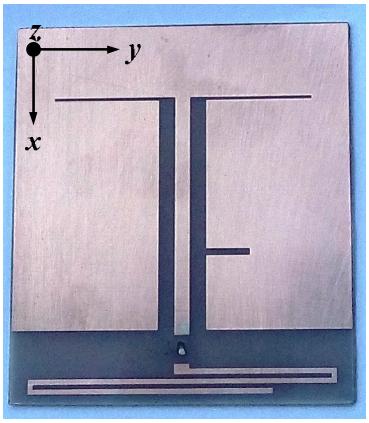

(b)

Figure 6.1: (a) Geometry of proposed dual antenna with zoomed section of the feed connections and (b) fabricated prototype of proposed dual tag antenna.

Table 6.1 Optimized shape parameters of the proposed RFID antenna

Antenna parameter	Value (mm)	Antenna parameter	Value (mm)	Antenna parameter	Value (mm)
Lx1	25.5	Ly1	80	t1	0.7
Lx2	70	Ly2	49	t2	1.5
Lx3	9	Ly3	15.5	t3	3.5
Lx4	50	Ly4	16	t4	3
Lx5	25.5	d	1.5	t5	3

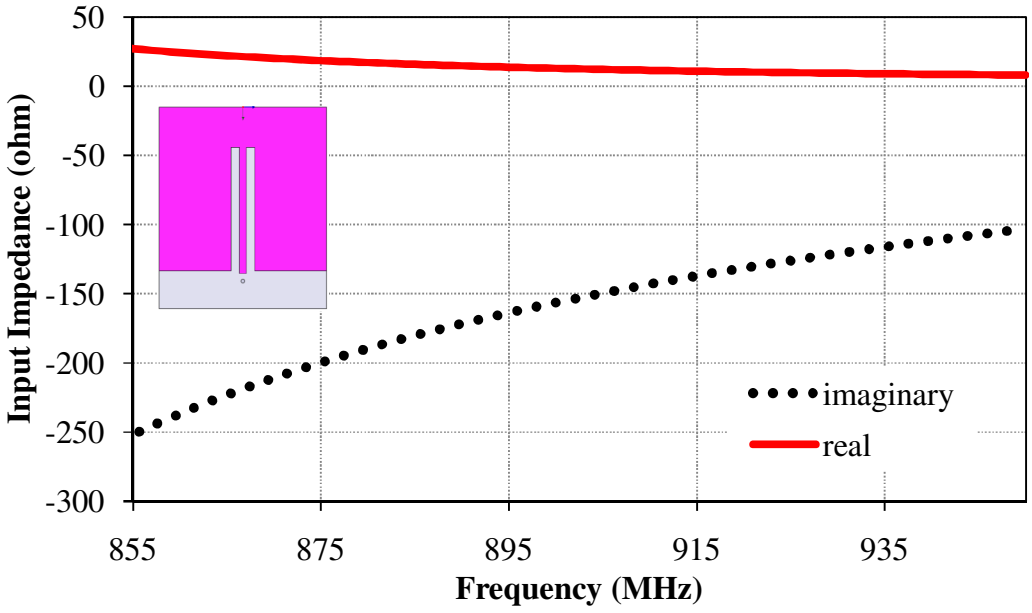

(a)

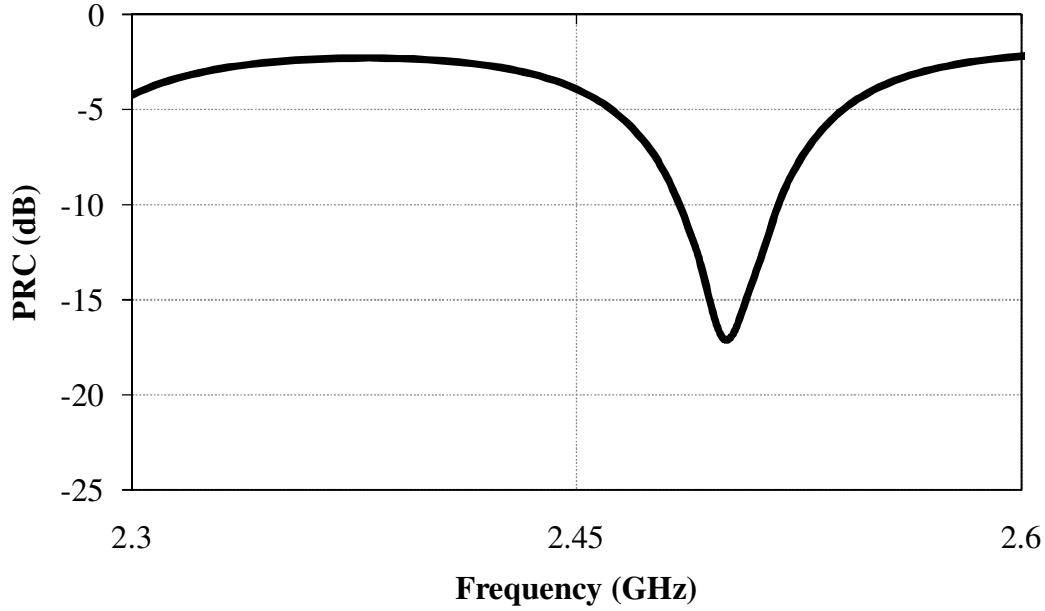

(b)

Figure 6.2: (a) input impedance of antenna at 915 MHz and (b) PRC of antenna at 2.45 GHz at step one of designing of antenna.

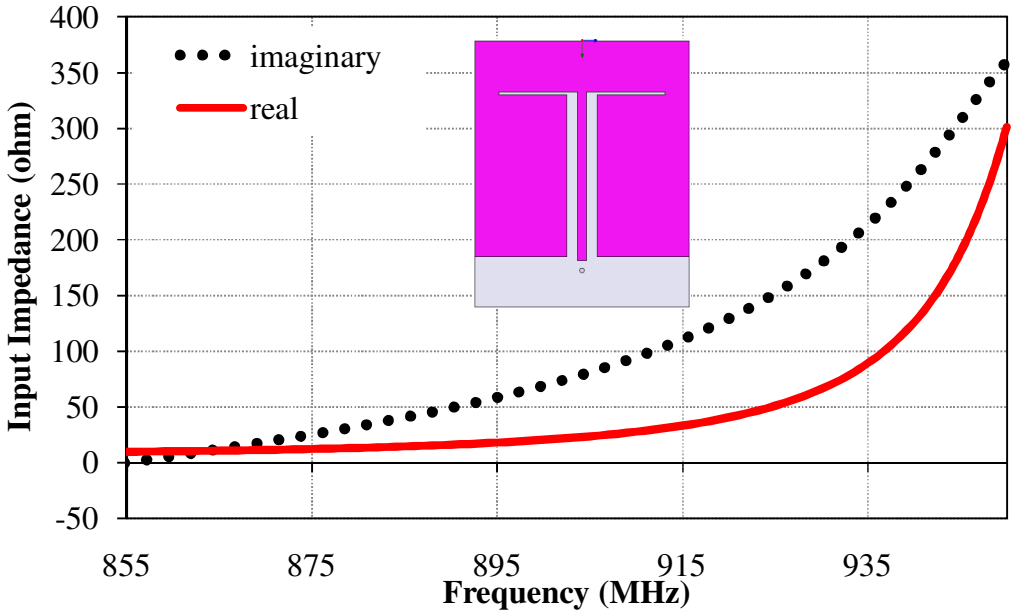

(a)

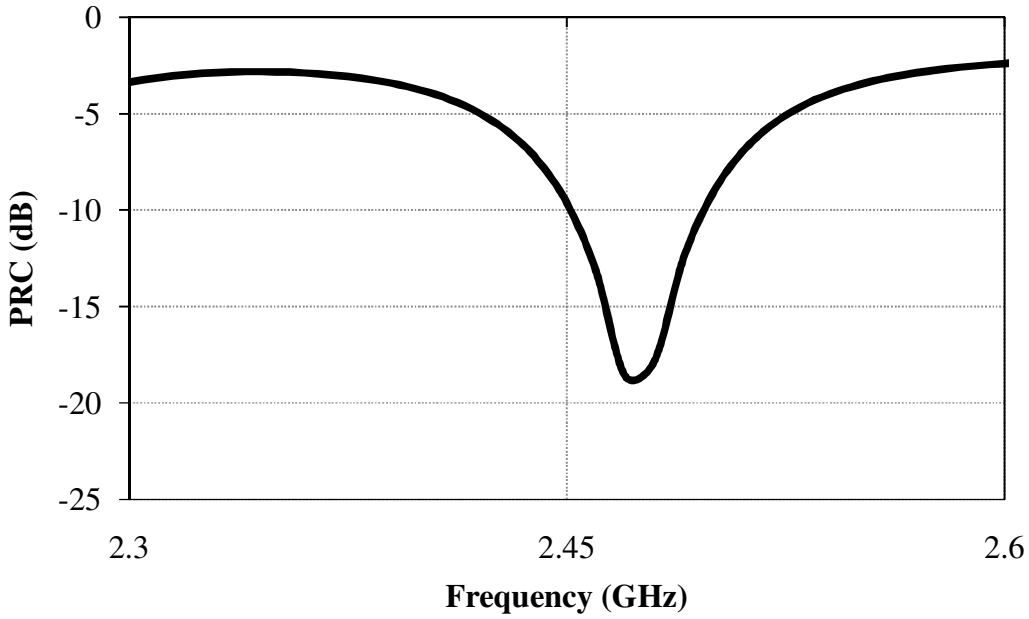

(b)

Figure 6.3: (a) input impedance of antenna at 915 MHz and (b) PRC of antenna at 2.45 GHz at second step of designing of antenna.

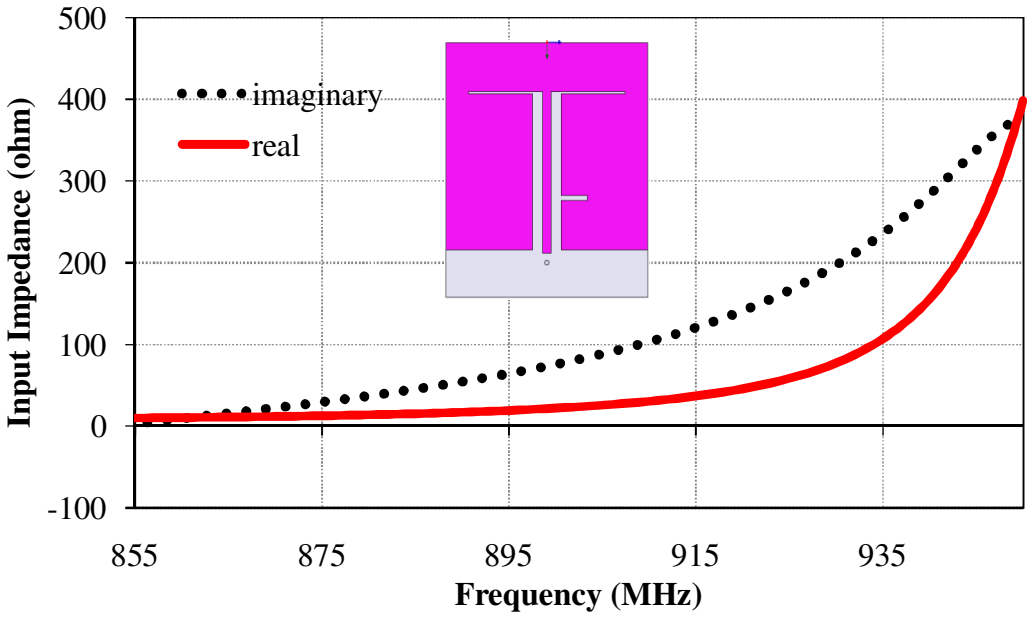

(a)

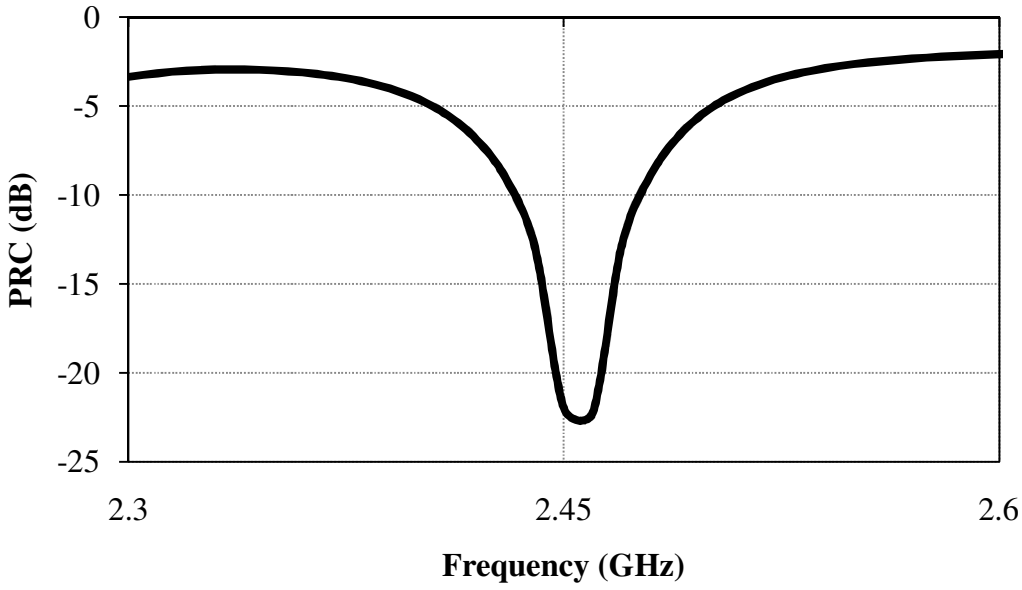

(b)

Figure 6.4: (a) input impedance of antenna at 915 MHz and (b) PRC of antenna at 2.45 GHz at third step of designing of antenna

6.3. Results and discussion

The presented tag antenna is designed for Impinj Monza Gen2 tag chip with input impedance of 33-j112Ω at 915 MHz [Monza4 Tag] and 50Ω at 2450 MHz. All the simulations are performed using the Ansys high frequency structure simulator (HFSS) [HFSS ver. 14.0].The optimized value of the shape parameters of the proposed antenna are shown in Table 6.1.

6.3.1. Parametric Study

Variations of simulated input impedance and power reflection coefficient (PRC) of receiving antenna at 915 MHz and 2450 MHz by varying *Lx*1 and *t*1 keeping optimized values for remaining parameters are presented in Figures 6.5-6.8. It is observed that the input impedance of the lower frequency band can be tuned with the length (*Lx*1) and width (*t*1) of the horizontal slit of inverted L-shaped and F-shaped slits so that complex conjugate of different RFID tag chip impedance can be achieved. Further, it is also observed from Figure 6.5 that for the optimum value of *Lx*1 and *t*1, the real and imaginary part of input impedance are 34Ω and j113Ω at 915 MHz. It is close proximity to the complex conjugate of the chip impedance i.e., 33-j113Ω, therefore maximum power will transfer to antenna which is also corroborated from the PRC variation shown in Figure 6.6. However, an insignificant effect of these parameters is observed on SHF band (Figures 6.7 and 6.8).

Variations of simulated input impedance of receiving antenna at 915 MHz and 2450 MHz by varying *t3* and *Ly2* keeping optimized values remaining parameters are presented in Figures 6.9 and 6.10. It is observed that the input impedance of the antenna at lower and higher frequency band can be tuned with the parameters t3 and Ly2.

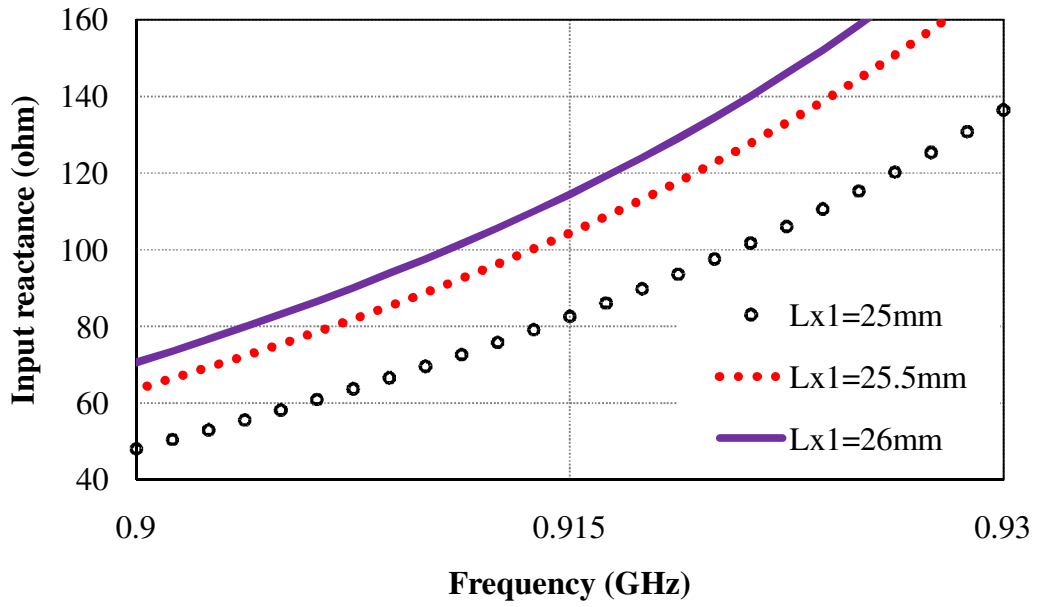
160
140
120
100
80
60
40
Input reactance (ohm)
0.9
0.915
0.93
Frequency (GHz)
Lx1=25mm
Lx1=25.5mm
Lx1=26mm

(a)

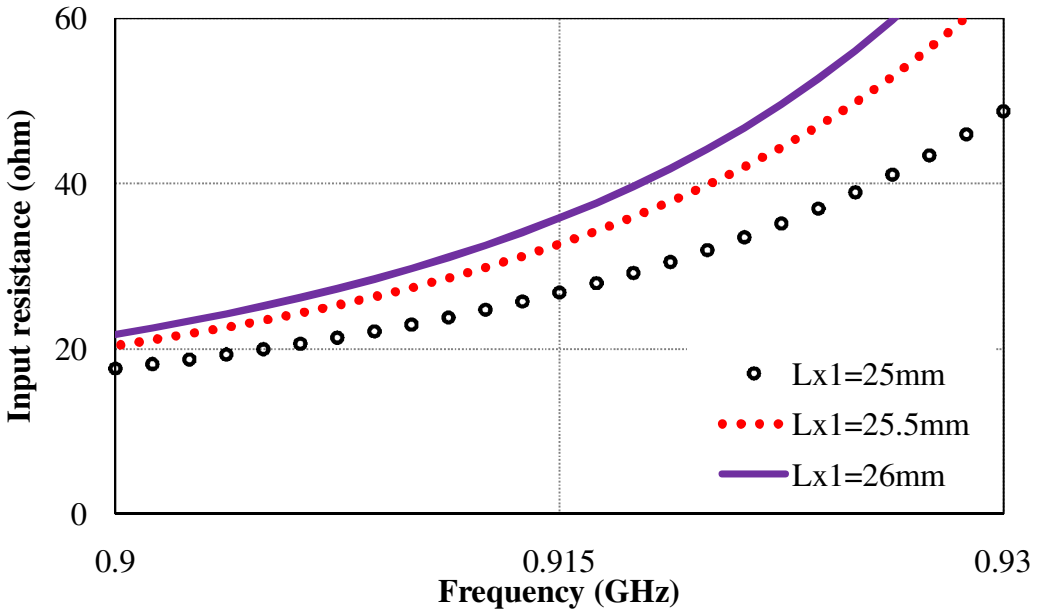
60
40
20
0
Input resistance (ohm)
0.9
0.915
0.93
Frequency (GHz)
Lx1=25mm
Lx1=25.5mm
Lx1=26mm

(b)

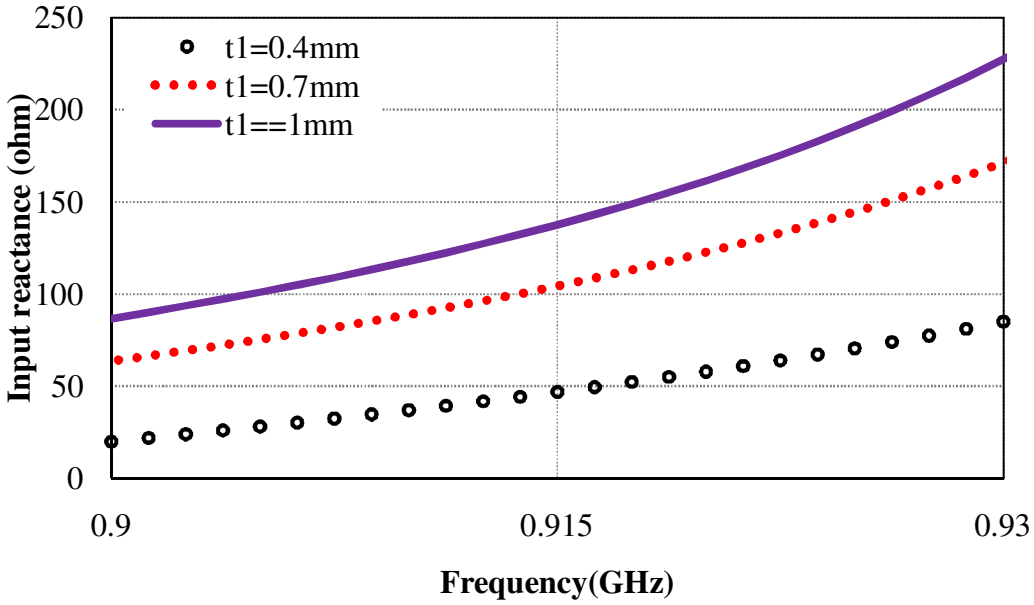

(c)

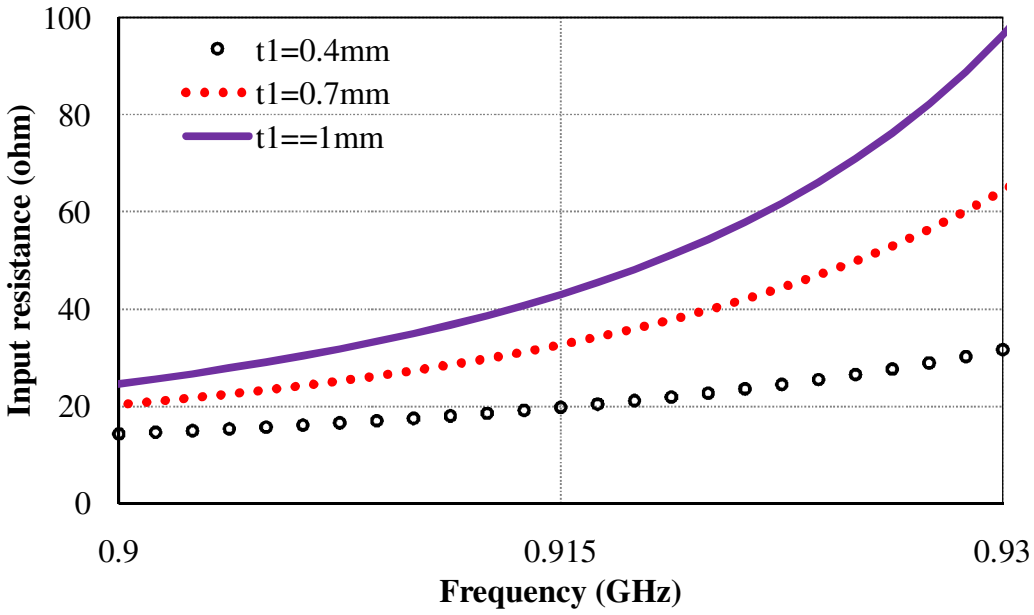

(d)

Figure 6.5: Simulated real and imaginary part of Input impedance of receiving antenna about UHF band by tuning: (a), (b) Lx_1 and (c), (d) t_1

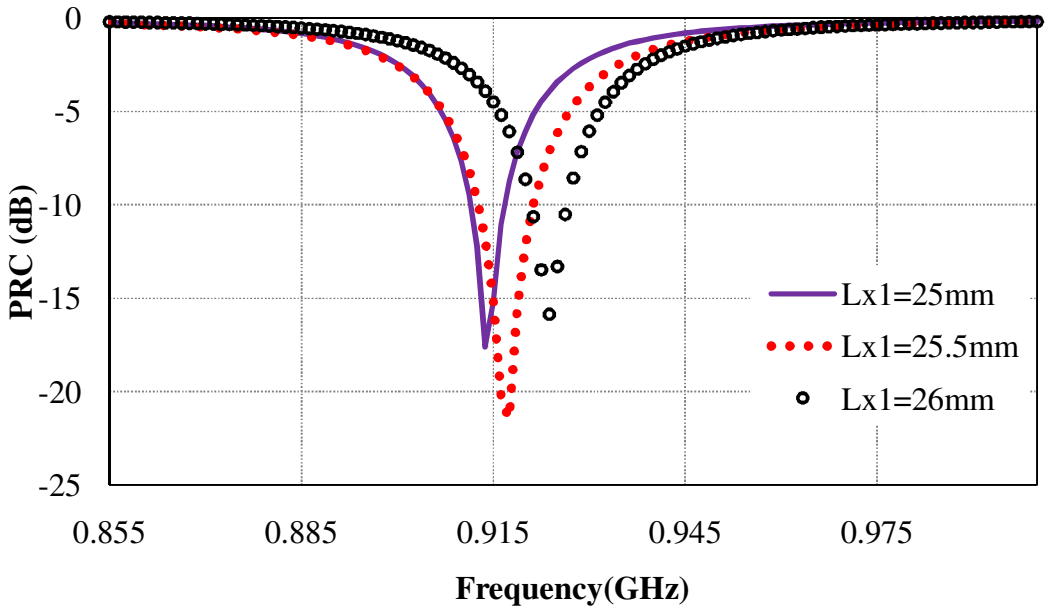

(a)

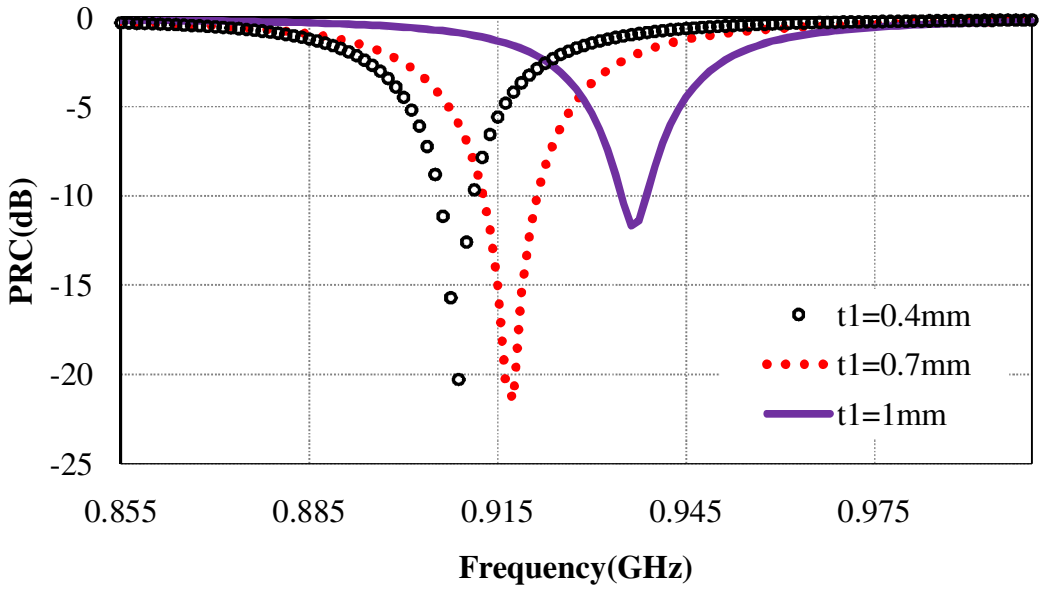

(b)

Figure 6.6: Simulated power reflection coefficient of receiving antenna about UHF band by tuning: (a) *Lx*1, and (b) *t*1.

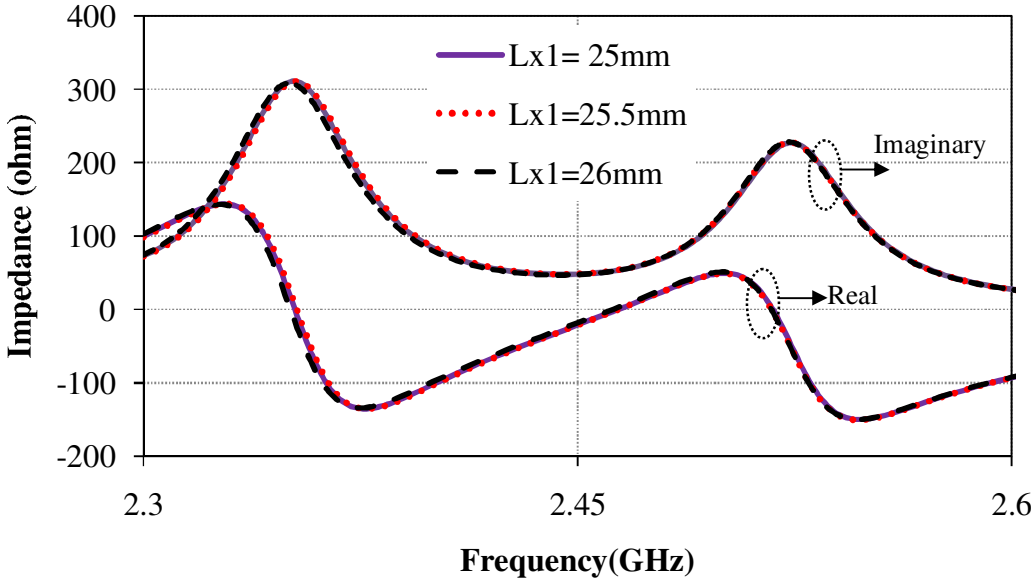

(a)

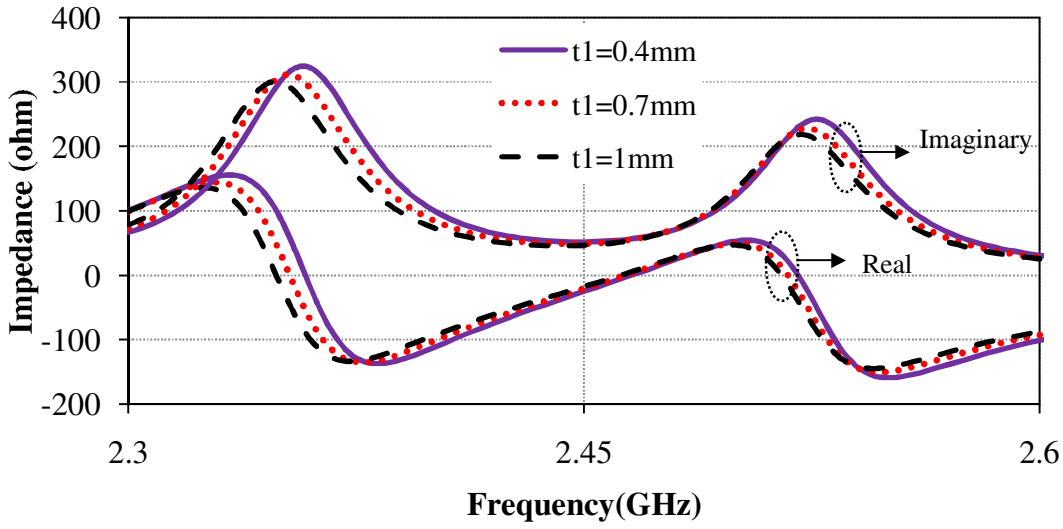

(b)

Figure 6.7: Simulated input impedance of receiving antenna about SHF band by tuning: (a) *Lx*1, and (b) *t*1.

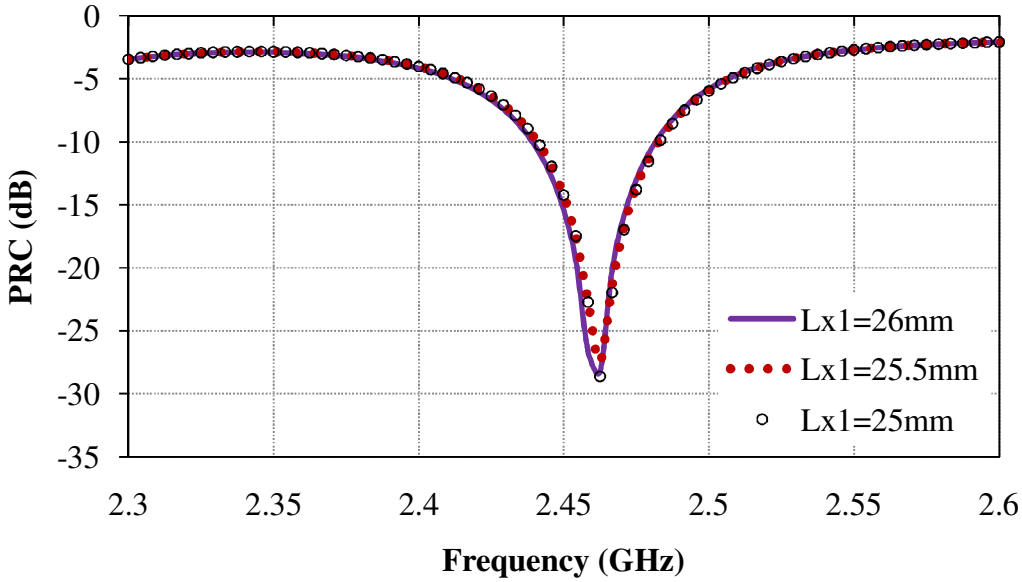

(a)

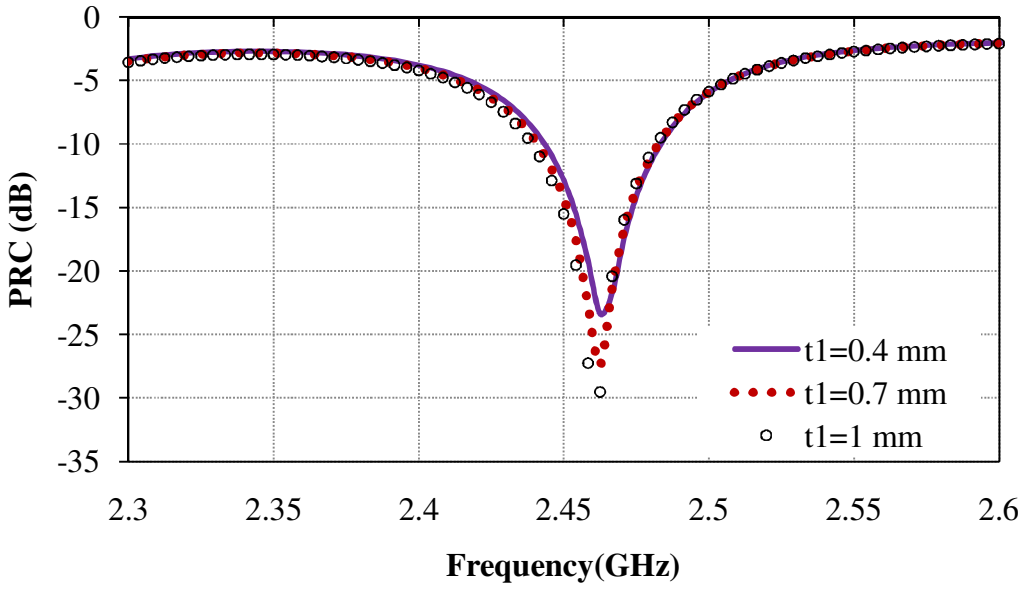

(b)

Figure 6.8: Simulated power reflection coefficient of receiving antenna about SHF band by tuning: (a) *Lx*1, and (b) *t*1.

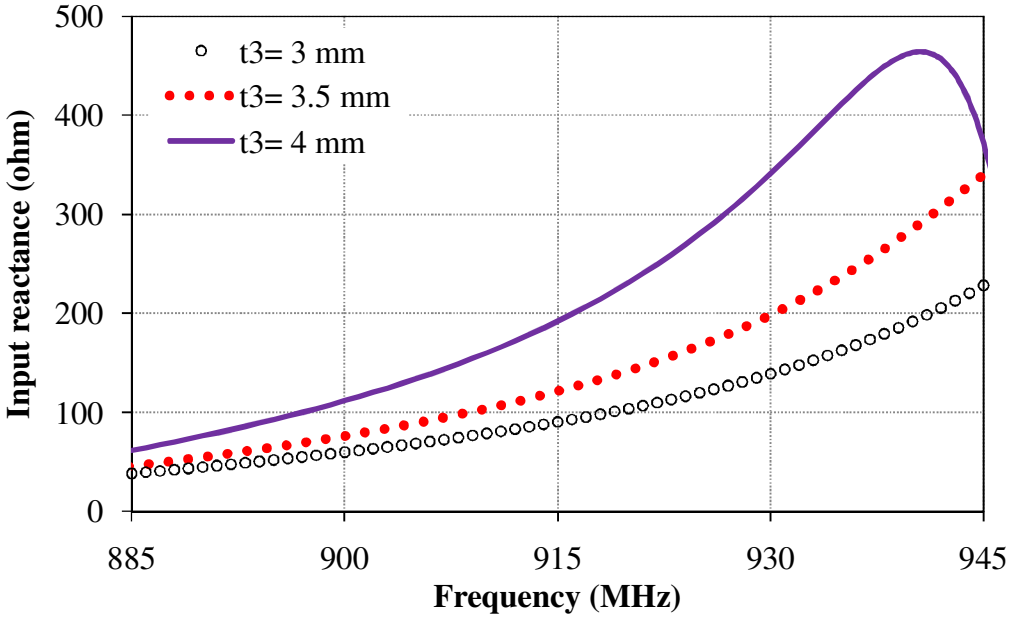
500
400
300
200
100
0
Input reactance (ohm)
t3= 3 mm
t3= 3.5 mm
t3= 4 mm
885
900
915
930
945
Frequency (MHz)

(a)

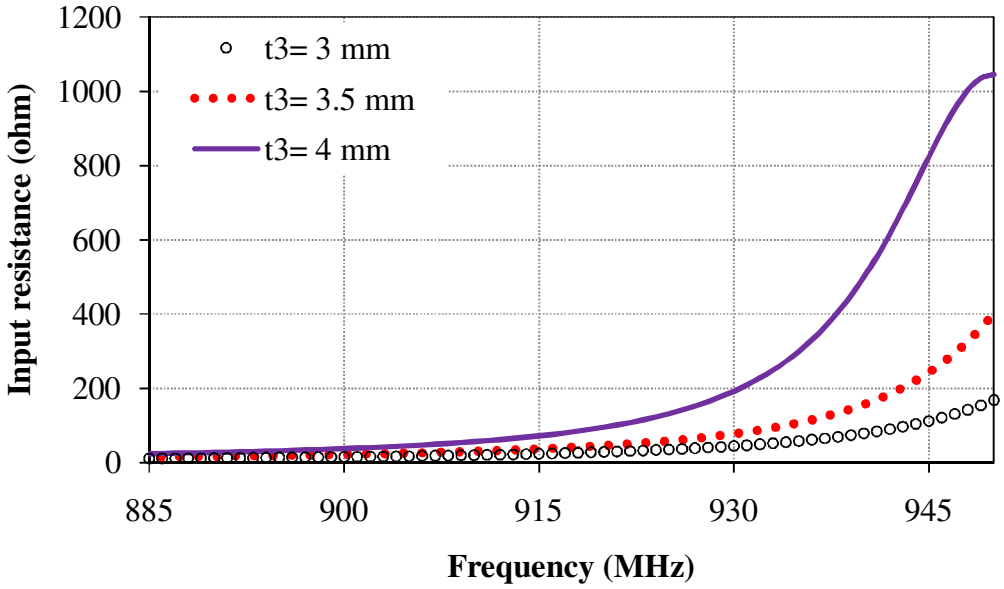
1200
1000
800
600
400
200
0
Input resistance (ohm)
t3= 3 mm
t3= 3.5 mm
t3= 4 mm
885
900
915
930
945
Frequency (MHz)

(b)

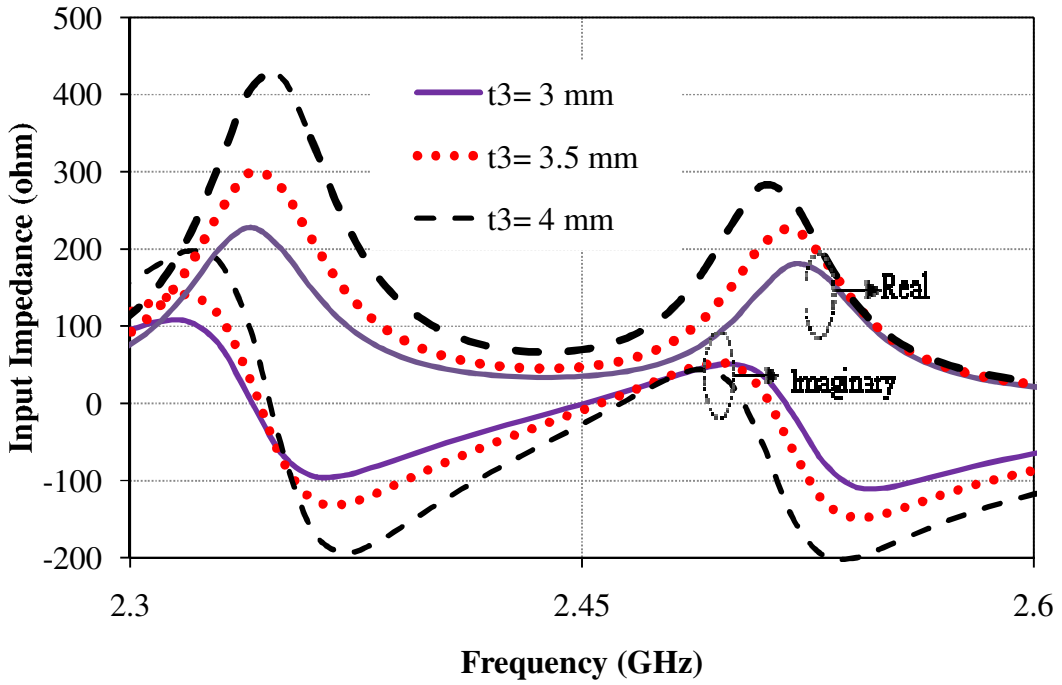

(c)

Figure 6.9: Simulated (a) input reactance at 915 MHz, (b) input resistance at 915 MHz, and (c) PRC at 2.45 GHz of receiving antenna by tuning t3

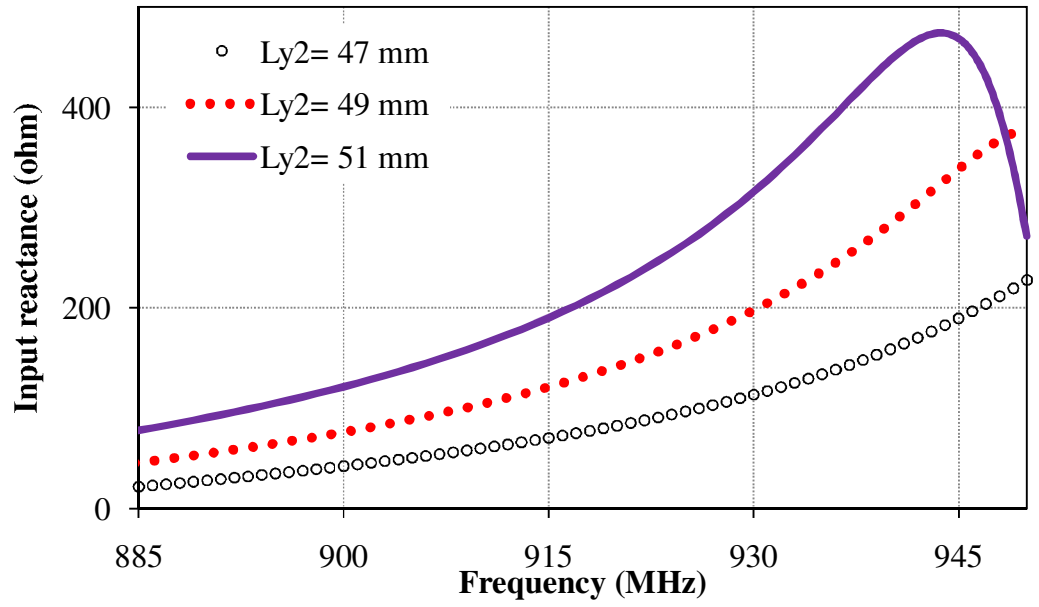

(a)

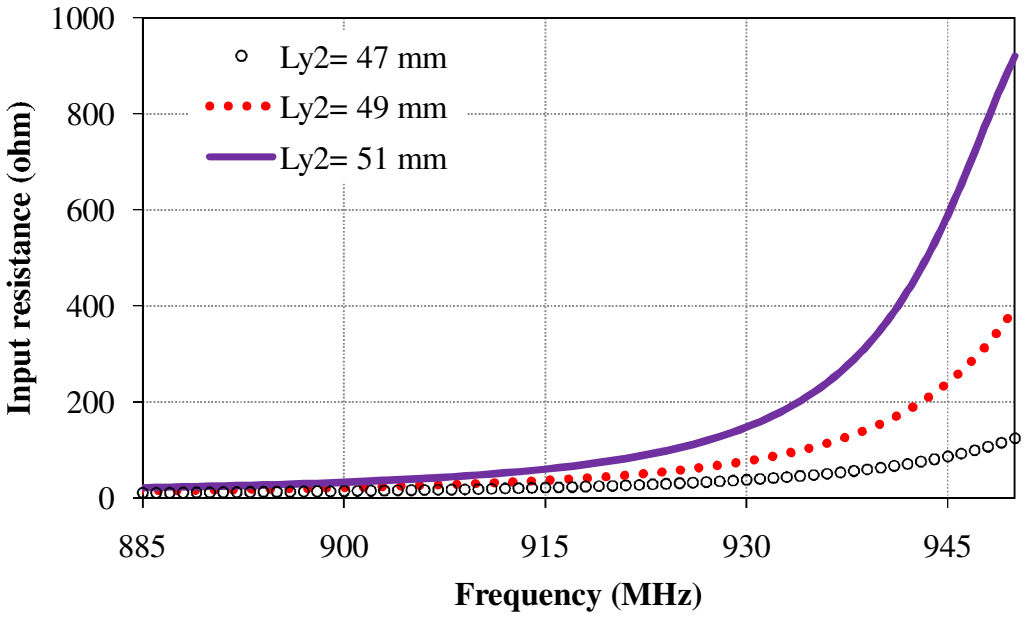

(b)

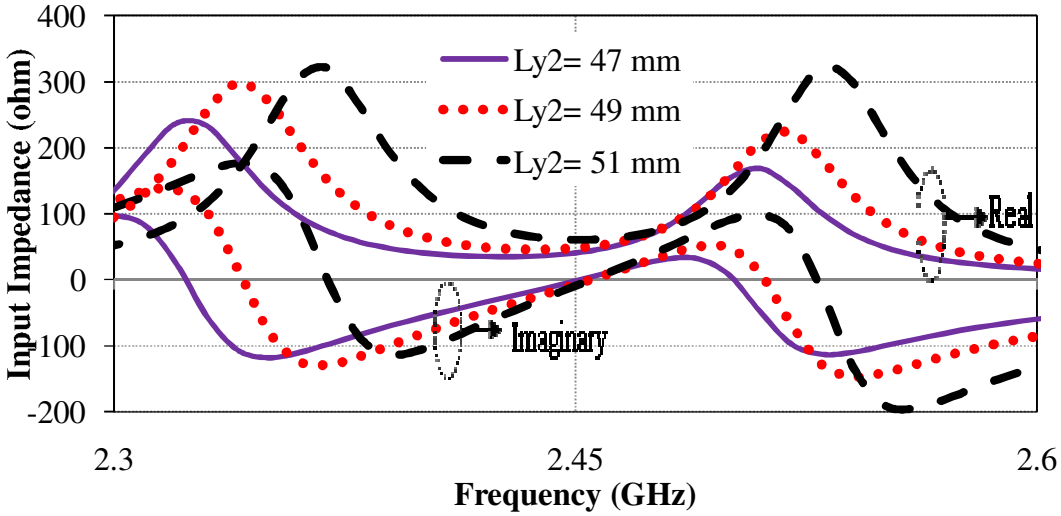

(c)

Figure 6.10: Simulated (a) input reactance at 915 MHz, (b) input resistance at 915 MHz, and (c) PRC at 2.45 GHz of receiving antenna by tuning Ly2

Figure 6.11 shows the variation of the input impedance and power reflection coefficient of the antenna at 2450 MHz by tuning *Lx*3 keeping optimized values of remaining parameters. It is observed that the real part of impedance approaches to 50Ω whereas imaginary part of the impedance

approaches to 0Ω when Lx3 is equal to 9 mm which is responsible for the good impedance matching with the tag chip. Due to which maximum power will transfer from chip to antenna which is corroborated from the PRC plot of Figure 6.11 (b). Figure 6.12 shows the input impedance and power reflection coefficient at 915 MHz by tuning same parameter *Lx*3 by keeping optimized values of remaining parameters. It is observed that the real part of the impedance approaches to 33Ω whereas imaginary part deteriorates from 113Ω to 104.6Ω. Therefore, the slit parameters are very sensitive for the optimization of the input impedance of the receiving antenna.

Figures 6.13 and 6.14 show the variation of the input impedance of antenna at 915 MHz (UHF band) and 2450 MHz (SHF band) by tuning Ly3 and t2 keeping optimized values of remaining parameters. The result shows that Ly3 and t2 have more effects on higher frequency side of the input impedance variation.

Figure 6.15 and 6.16 show the variation of imaginary part of the input impedance with frequency for the backscattering antenna by varying the *Lx*4 and t5, at 915 MHz (UHF band), while the receiving antenna is conjugately matched with the chip. To satisfy the condition of backscattering, the value of reactance of the backscattering antenna should be close to zero for maximum differential RCS. It is observed that the reactance value of the backscatter antenna (Antenna II) is close to zero (-4.3Ω) for UHF band. To investigate the effect of *Lx*4 on the input impedance of receiving antenna (Antenna-I) at UHF band, Figure 6.17 is plotted. It is observed that input impedance of the Antenna-I is independent on the *Lx*4. This indicates that both Antenna-I and Antenna-II work independently at UHF band.

Figure 6.18 shows the isolation between receiving and backscattering antenna at UHF band. It is observed that the value of isolation at 915 MHz is better than -20 dB.

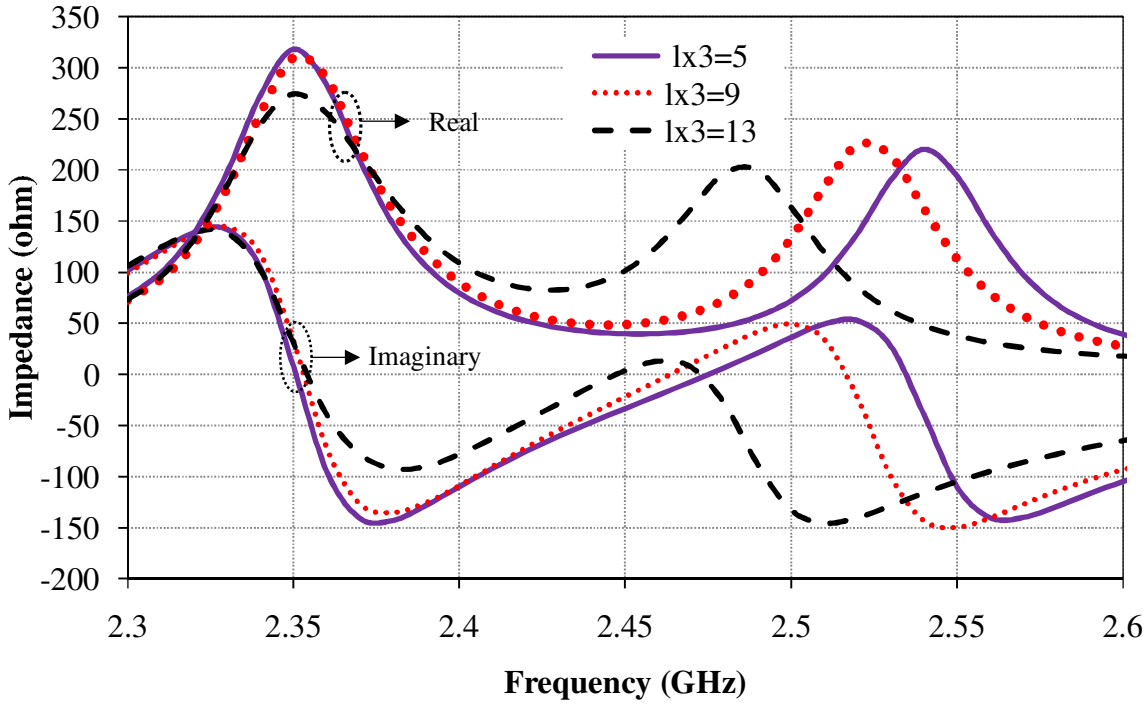

(a)

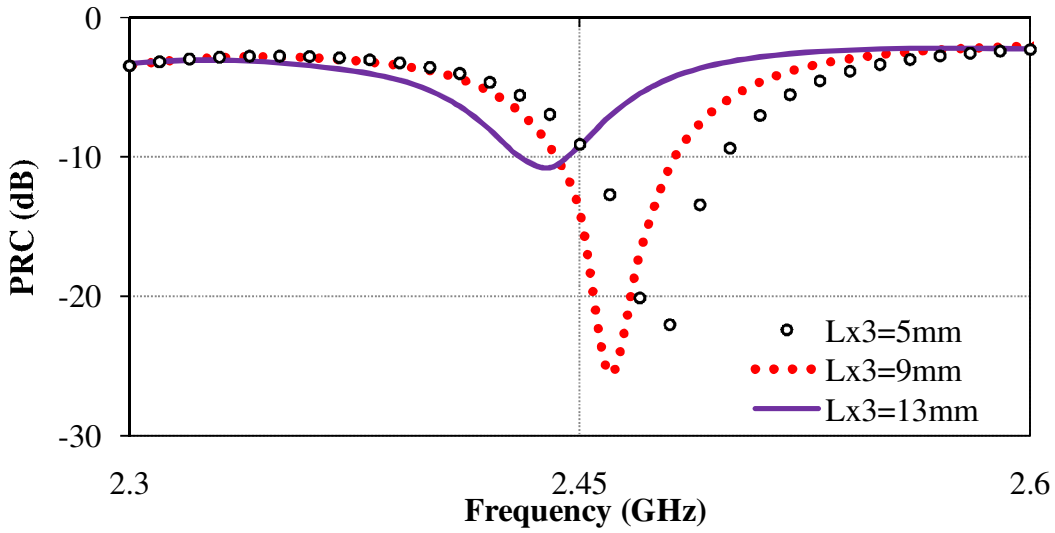

(b)

Figure 6.11: Simulated (a) Impedance and (b) Power Reflection Coefficient variation of Antenna-I by tuning *Lx*3 at 2.45 GHz.

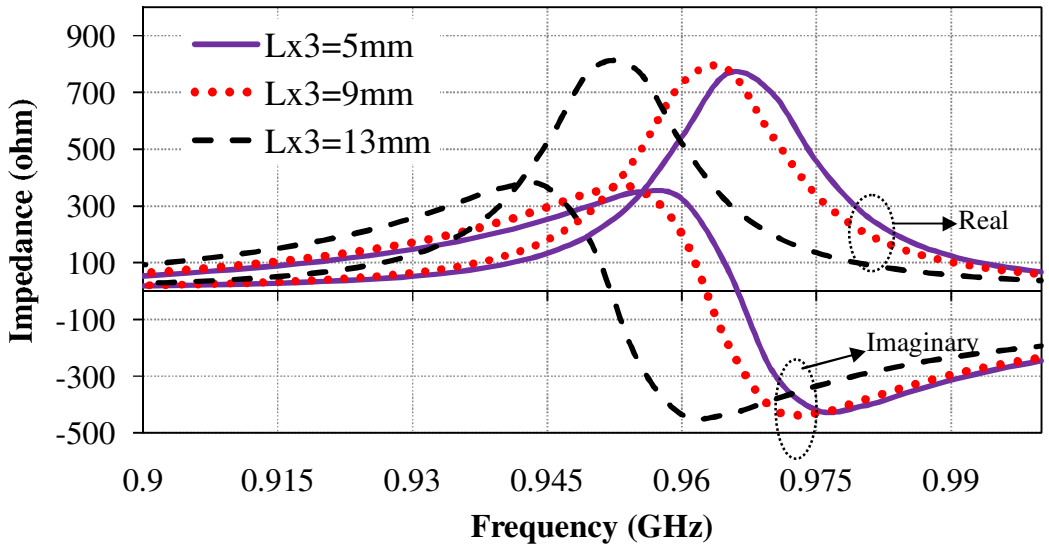

(a)

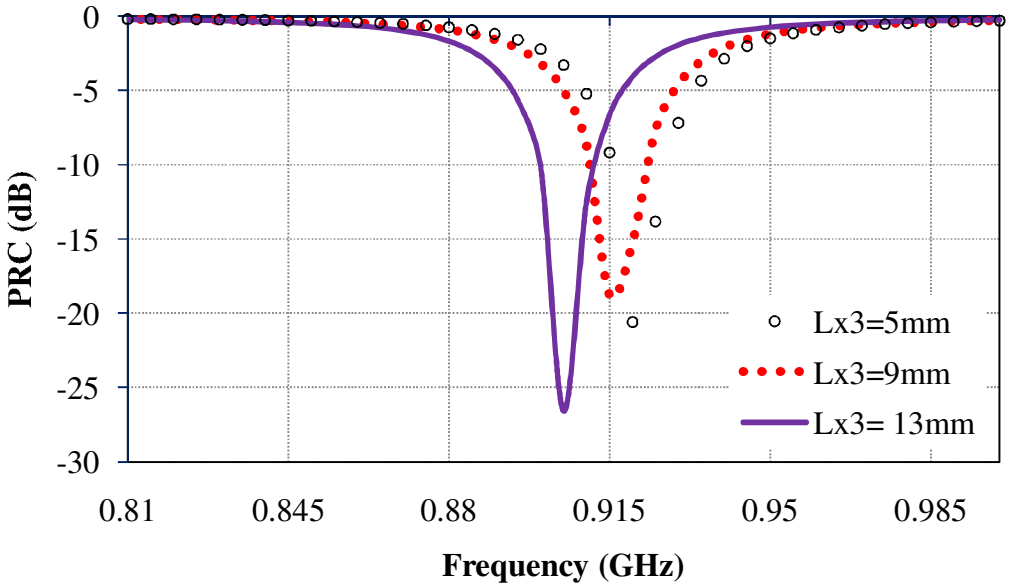

(b)

Figure 6.12: Simulated (a) impedance and (b) power reflection coefficient of antenna I, by tuning the Lx3 at 915 MHz.

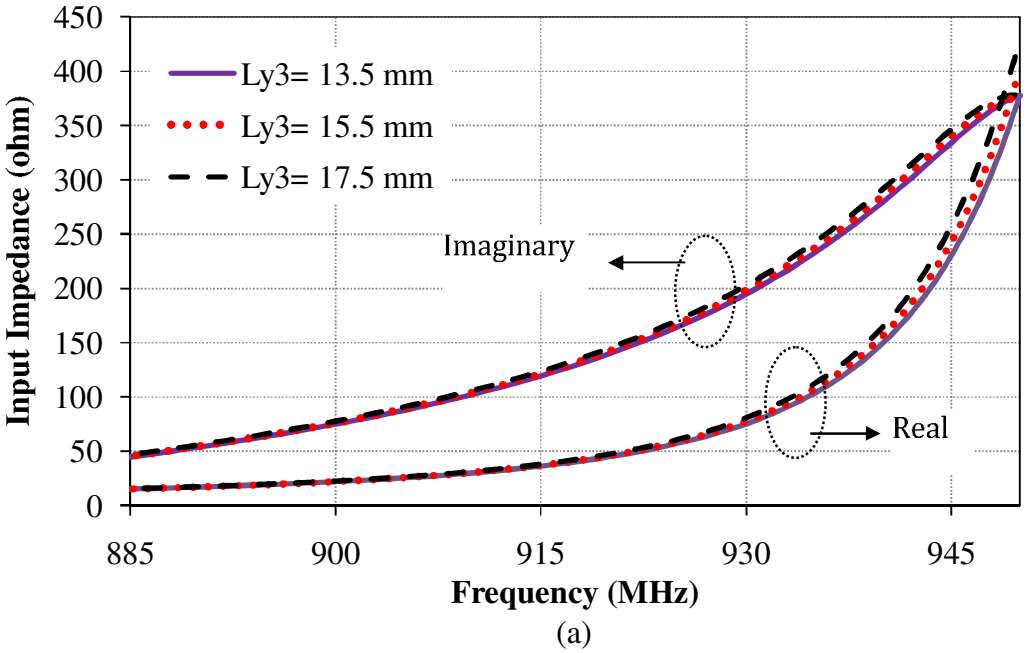

(a)

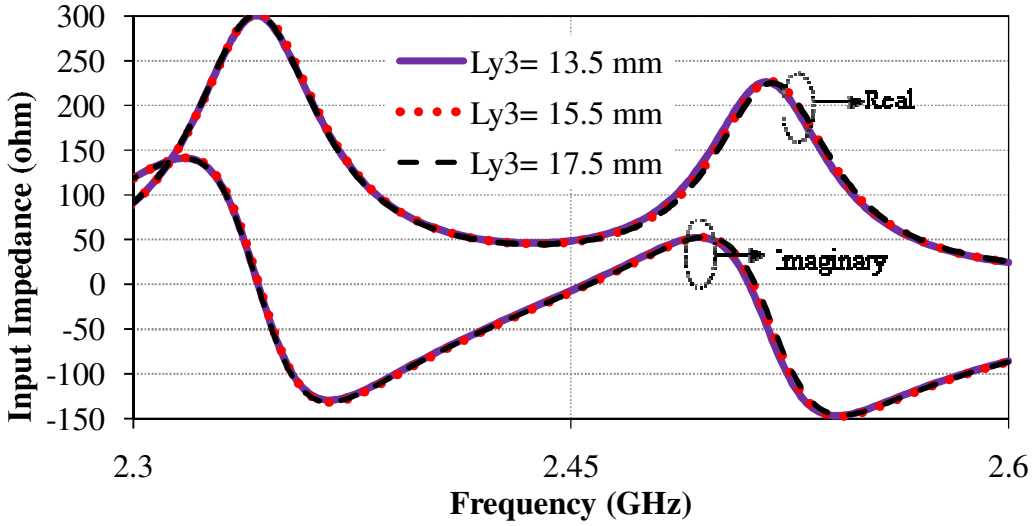

(b)

Figure 6.13: Simulated input impedance variation for (a) UHF band and (b) SHF band of Antenna-I by tuning *Ly*3.

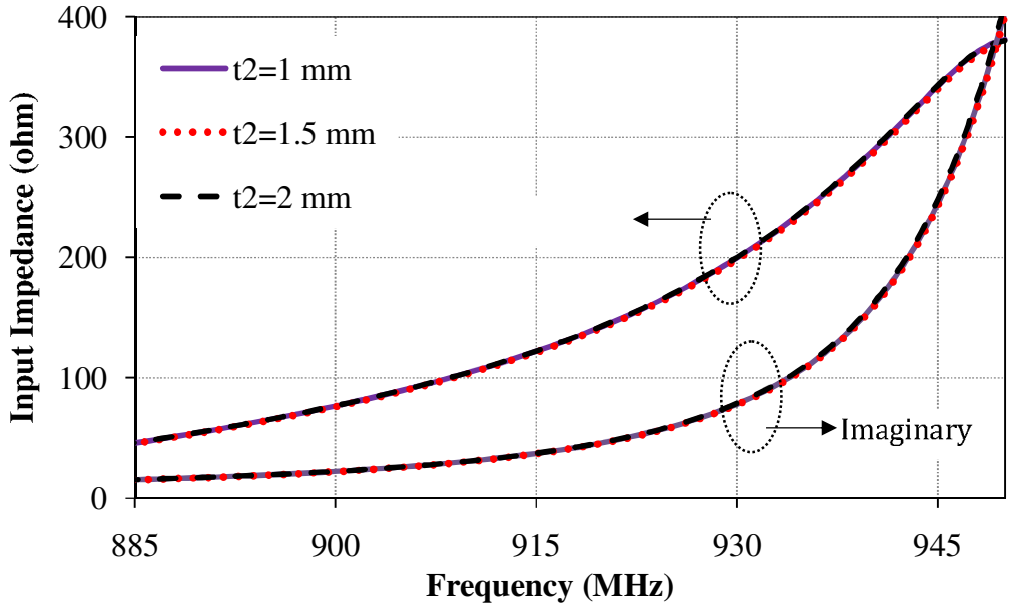

(a)

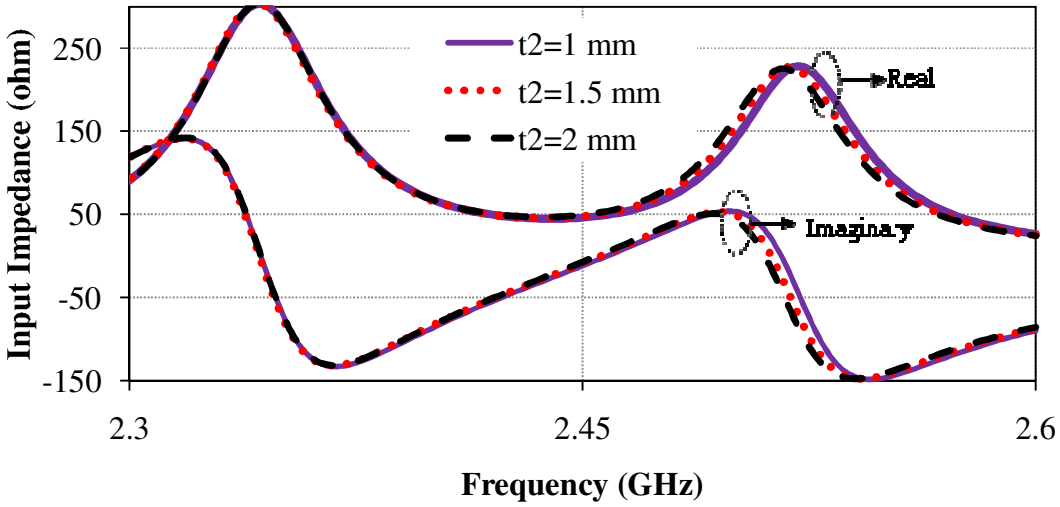

(b)

Figure 6.14: Simulated input impedance variation for (a) UHF band and (b) SHF band of Antenna-I by tuning *t2*.

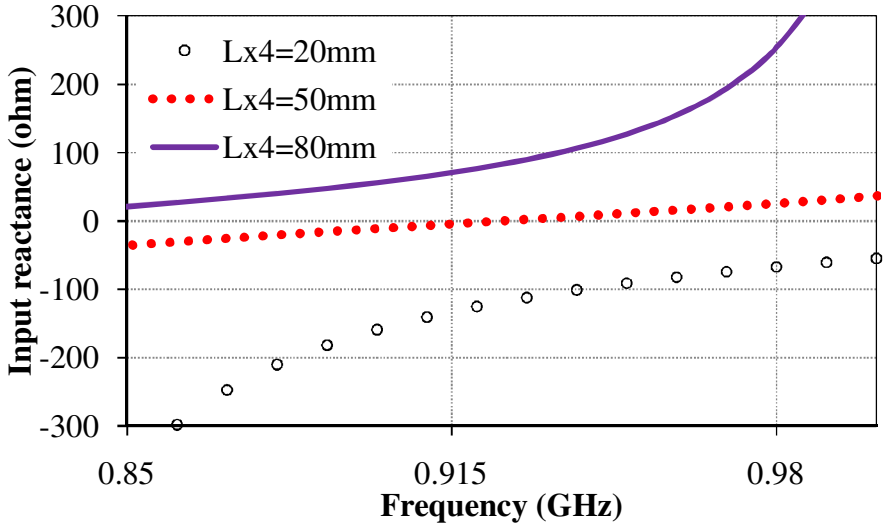

Figure 6.15: Simulated input reactance of backscattering antenna by tuning the Lx4.

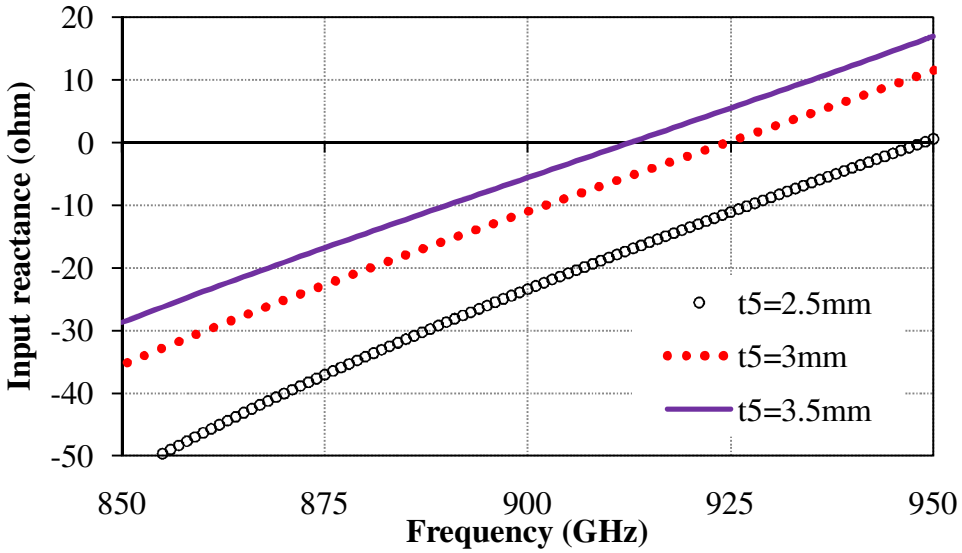

Figure 6.16: Simulated input reactance of backscattering antenna by tuning the *t5*

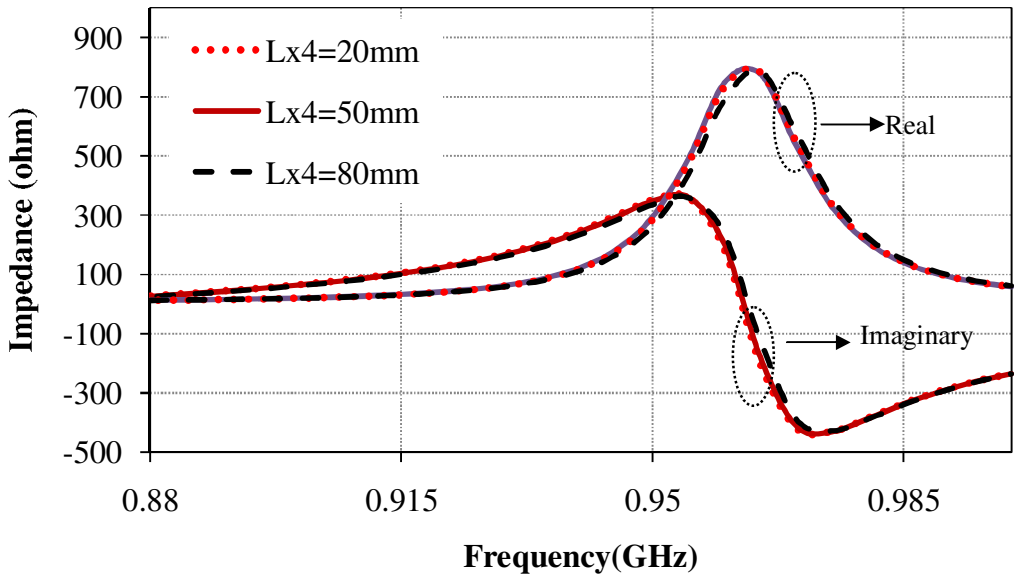

(a)

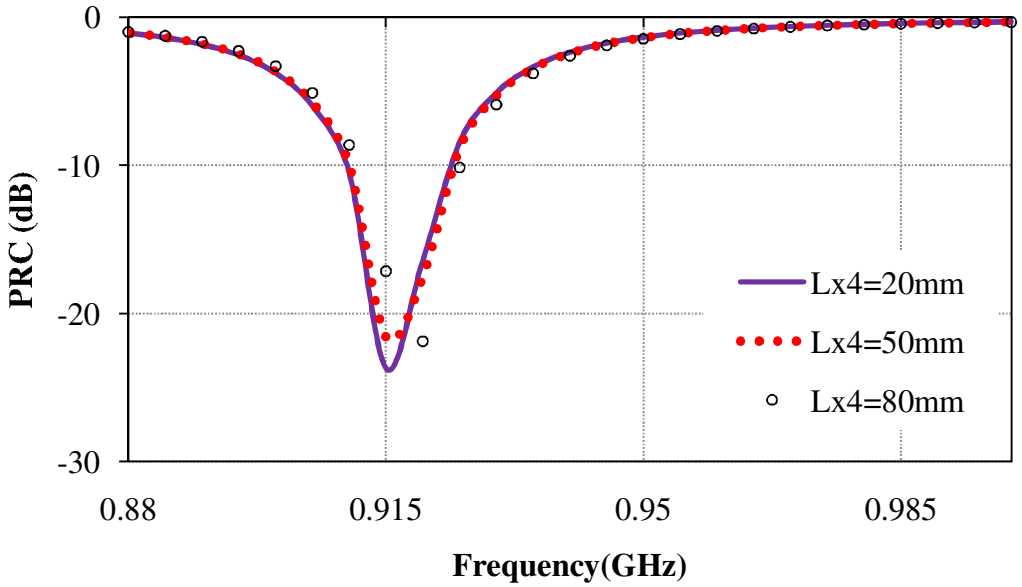

(b)

Figure 6.17: Simulated (a) input impedance and (b) power reflection coefficient variation of receiving antenna by tuning *Lx*4.

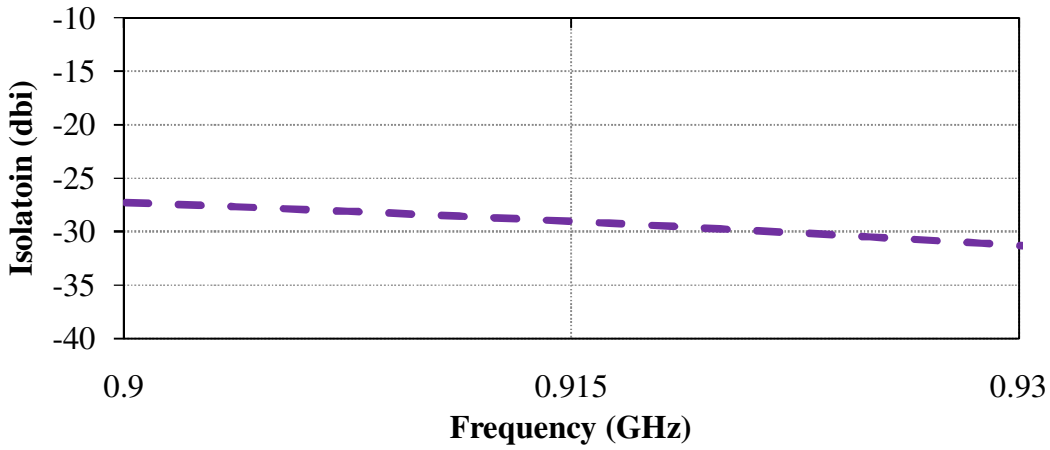

Figure 6.18: Isolation between receiving and backscattering antenna at 915MHz.

6.3.2. Simulation and Measurement Results

The *S*-parameters of the presented antenna is measured using differential probe method as described earlier in chapters two and three. Further, the measured *S*-parameters are used to calculate measured differential input impedance. After that with the help of differential input impedance, power reflection coefficient is calculated [Chen *et al.* (2011)a]. Figure 6.19 shows the measurement setup to measure the S_{11} of the presented antenna.

Figure 6.19: Measurement setup for S_{11} measurement

Figure 6.20 shows the simulated and measured results of the input impedance of receiving antenna (Antenna-I) for UHF band. The measured and simulated input impedance at 915 MHz are observed as 47.8+j164Ω and 32.64+j104Ω, respectively. The simulated results are close to the complex conjugate of the chip impedance (33-j112Ω) whereas the variation in the measured result is obtained may be due to the fabrication tolerance of the differential probe and gap between the probe ends. Figure 6.21 shows the simulated and measured results of power reflection coefficient of Antenna-I for UHF and SHF bands. The simulated and measured input reactance of backscattering antenna (Antenna-II) for UHF band is shown in Figure 6.22. The simulated and measured results show reactance of the Antenna-II are -4.3Ω and -7.1Ω, respectively, which are close to zero impedance to provide maximum differential RCS for improved read range. The simulated and measured results are in agreement with respect to 2450 MHz whereas some variations are observed at 915 MHz which may be due to fabrication and calibration errors of the differential probe with the antenna.

The read range of the RFID tag antenna is proportional to the differential radar cross section (RCS) (Δσ) of an antenna under two different impedance states during the backscattering operation [Chen *et al.* (2011)a]. The RCS of proposed dual Antenna for UHF band (impedance states: short-circuit; Z_L=0 and open-circuit; Z_L=∞) is compared with conventional single antenna structure (impedance states: short-circuit; Z_L=0 and conjugate match; Z_L=33-j112) in Figure 6.23. This value of Δσ in two states of the conventional antenna are between 23.15 and 18.75 dBsm at 915 MHz is observed as 4.39 dBsm (from Figure 6.23(a)). Furthermore, in the case of dual antenna structure Δσ between 23.15 and -40.47 dBsm at 915 MHz is observed as 63.62 dBsm. It is clear that Δσ increased from 4.39 to 63.62 dBsm at 915 MHz. The differential RCS (Δσ) in two states (open and short) of proposed dual-antenna structure at 915 MHz is increased, which results in enhancement of read range from 4.1 to 5.05 m as shown in Figure 6.24. It is also noticed that the Antenna-I of proposed dual-antenna structure is conjugate match and the backscattered antenna alternatively switch between open and short

circuits. Furthermore, the read range of Antenna-I for SHF is also presented in Figure 6.25. The read range at 2450 MHz is observed about 6 m.

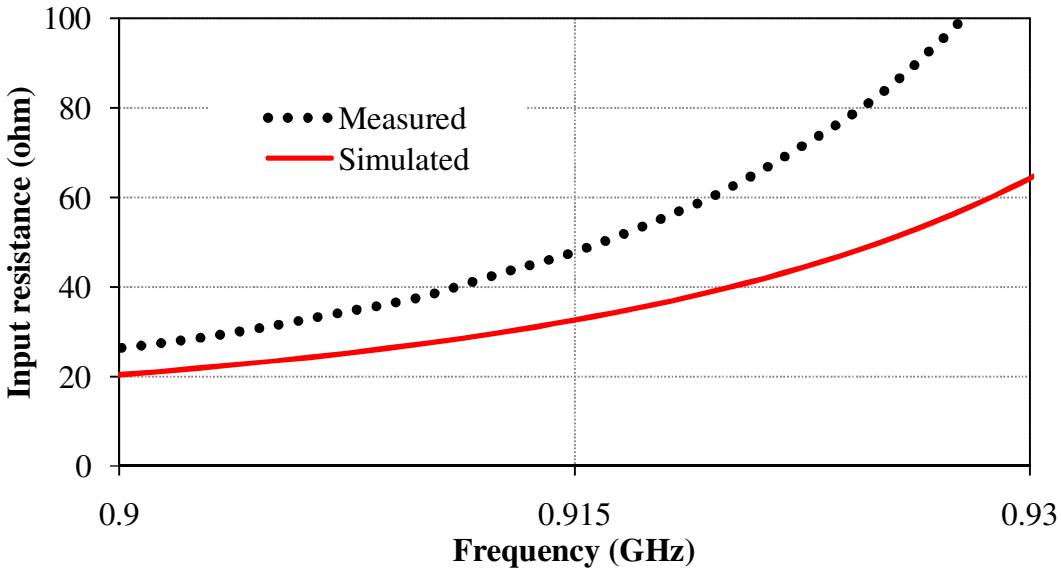

(a)

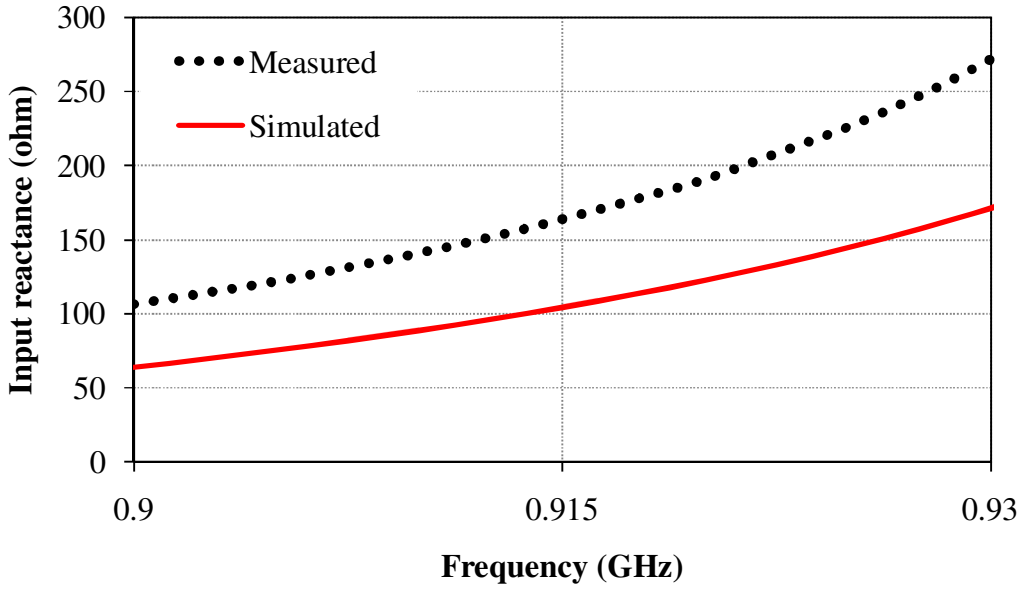

(b)

Figure 6.20: Simulated and measured input impedance variation of receiving antenna for UHF band (a) resistance and (b) reactance.

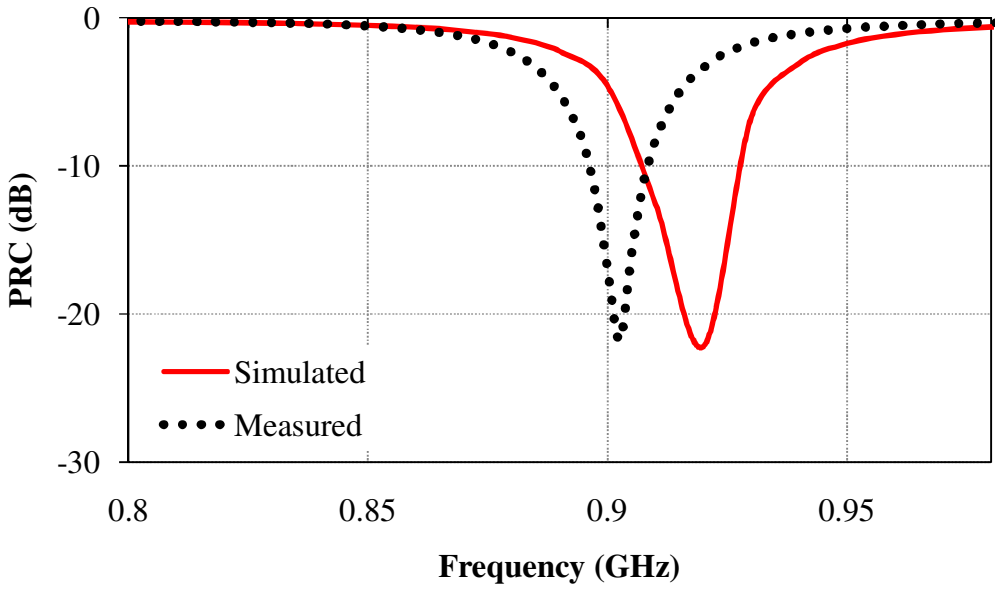

(a)

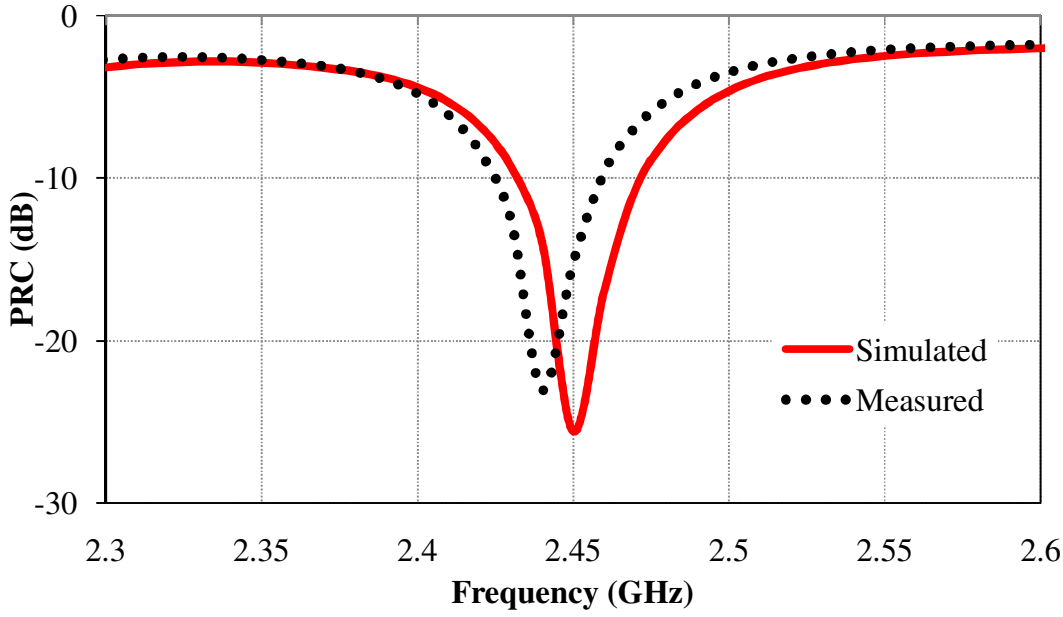

(b)

Figure 6.21: Simulated and measured power reflection coefficient variation of receiving antenna at (a) UHF band and (b) SHF band.

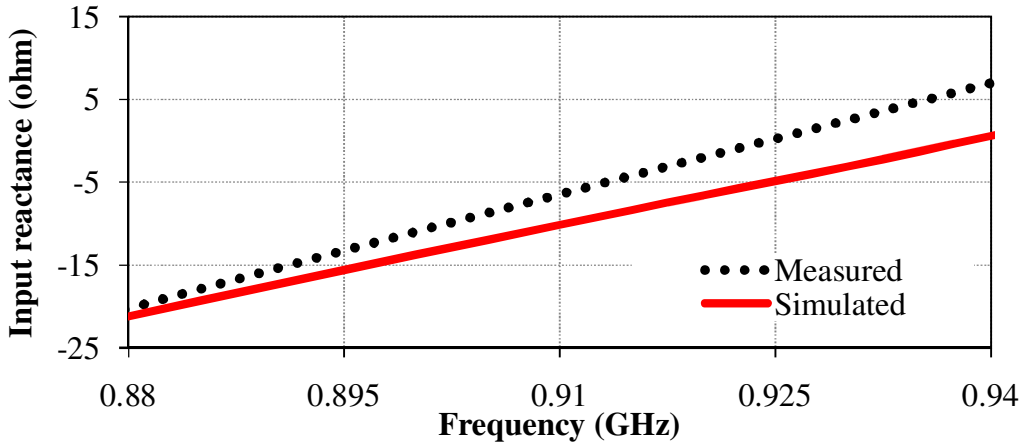

Figure 6.22: Simulated and measured input reactance of backscattering antenna for UHF band.

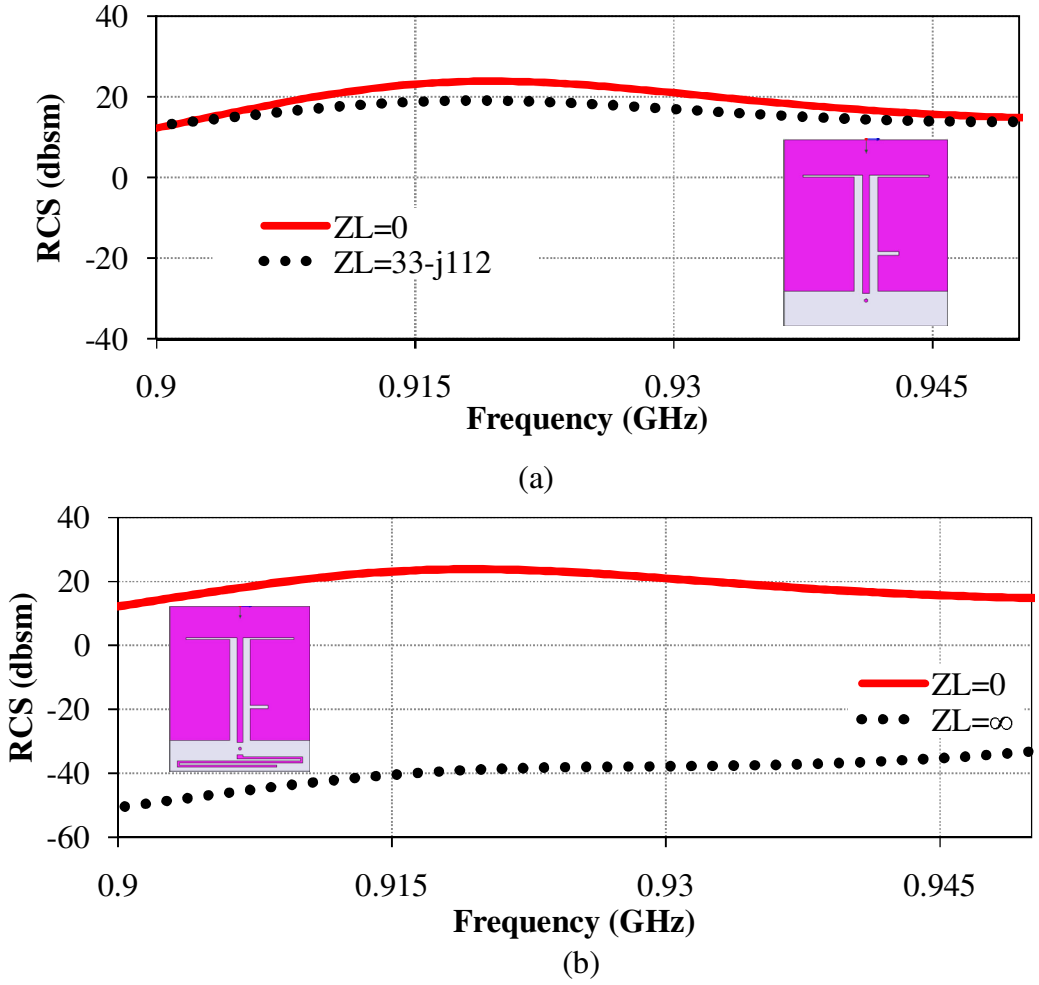

Figure 6.23: RCS variation of (a) conventional single antenna and (b) proposed antenna for UHF band.

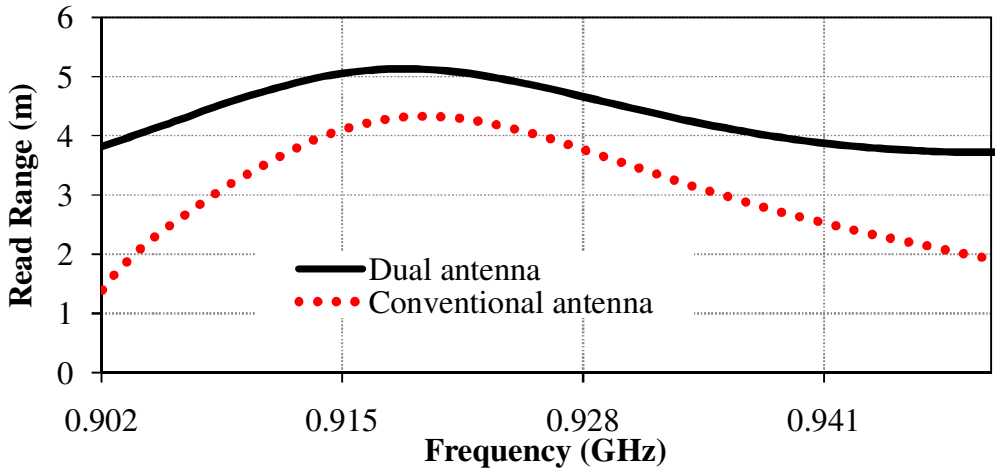

Figure 6.24: Read range comparison of conventional and proposed antenna for UHF band.

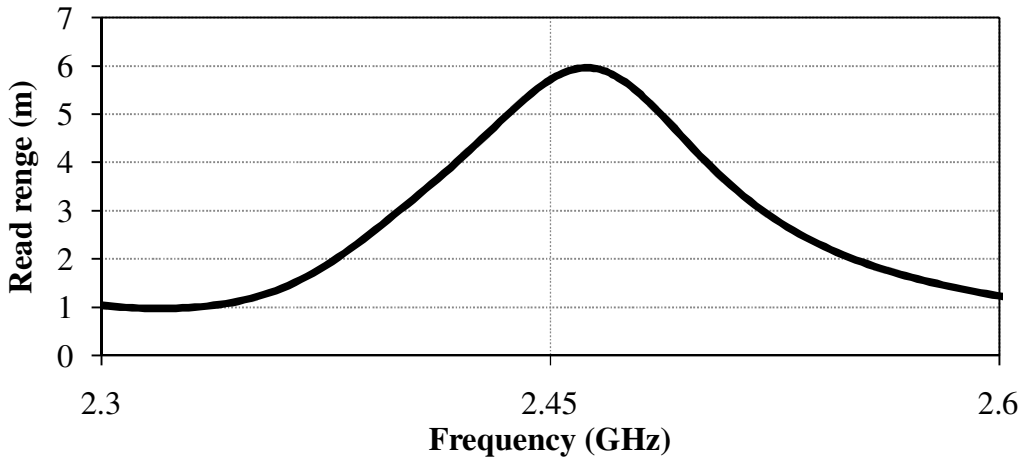

Figure 6.25: Read range variation of proposed antenna for SHF band.

Figure 6.26 shows the radiation patterns in both *xz*-plane and *yz*-plane of receiving (Antenna-I) of RFID tag at 915 MHz and 2450 MHz. It is observed that at 915 MHz, dumbbell shaped pattern is observed in both the planes. Whereas, at 2450 MHz, a null is observed about 180° in both the planes, while at other angular positions patterns are nearly stable.

Further, the RFID tag antenna is also investigated on a metallic surface of size 150×150 mm^2. The simulated power reflection coefficient and read range of antenna at 915 MHz and 2.45 GHz has been reported in Figure 6.27 and Figure 6.28. The results show that the characteristics of PRC and read range do not affect

severely. However, some shifting of the resonance is observed towards lower and higher frequency side for UHF and SHF, respectively, when antennas are placed on the metal sheet. Furthermore, the read range is also affected correspondingly. But, it still covers the 915 MHz and 2.45 GHz completely and will work effectively on these frequencies.

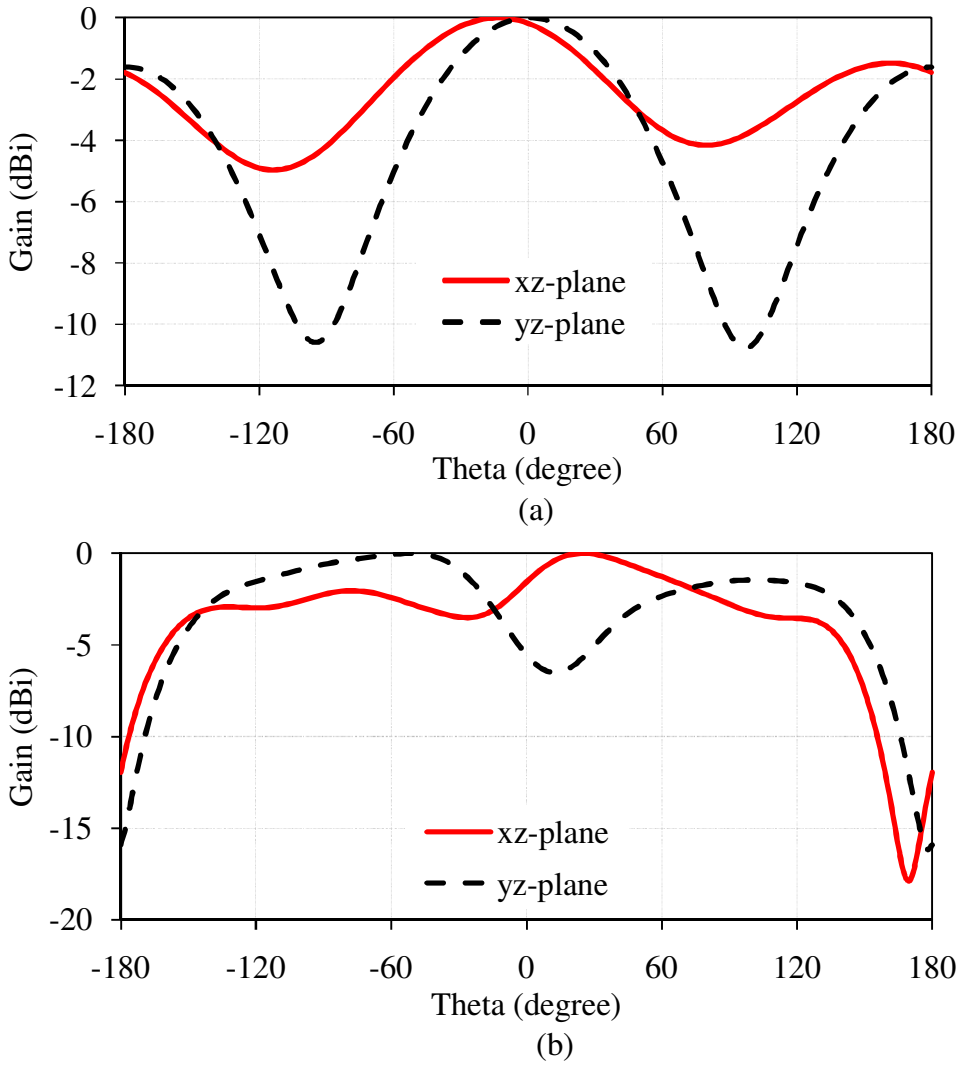

Figure 6.26: Radiation pattern of Antenna-I (receiving antenna) (a) 915 MHz and (b) 2450 MHz

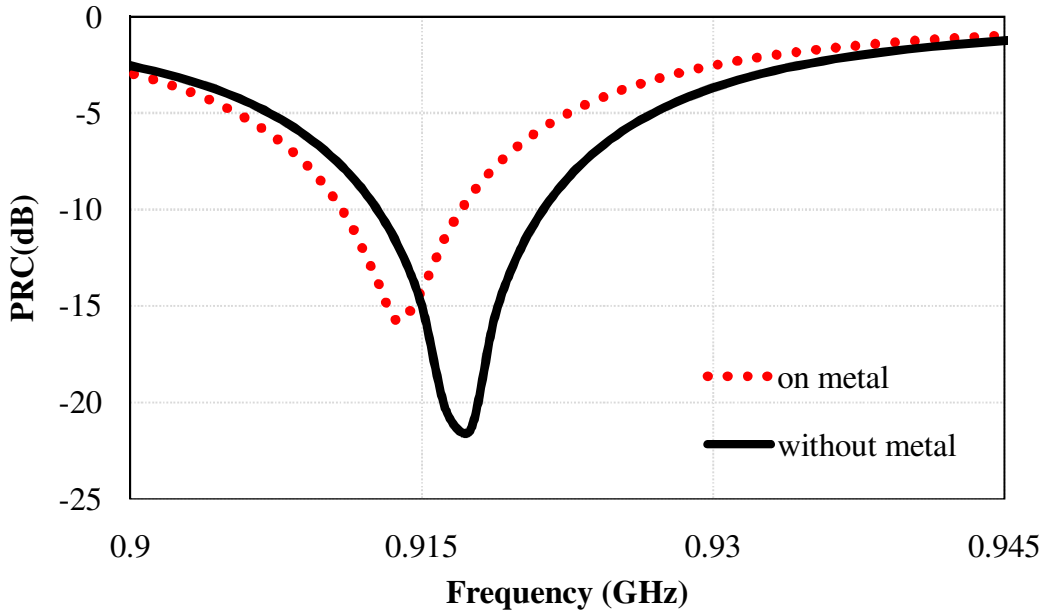

(a)

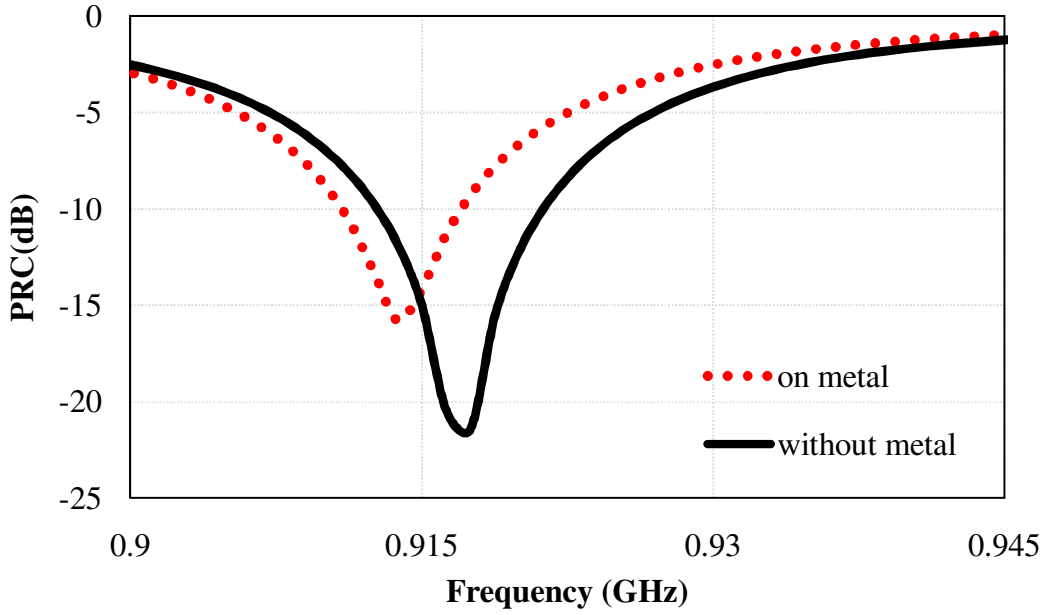

(b)

Figure 6.27: Simulated (a) power reflection coefficient and (b) read range of antenna in 915 MHz

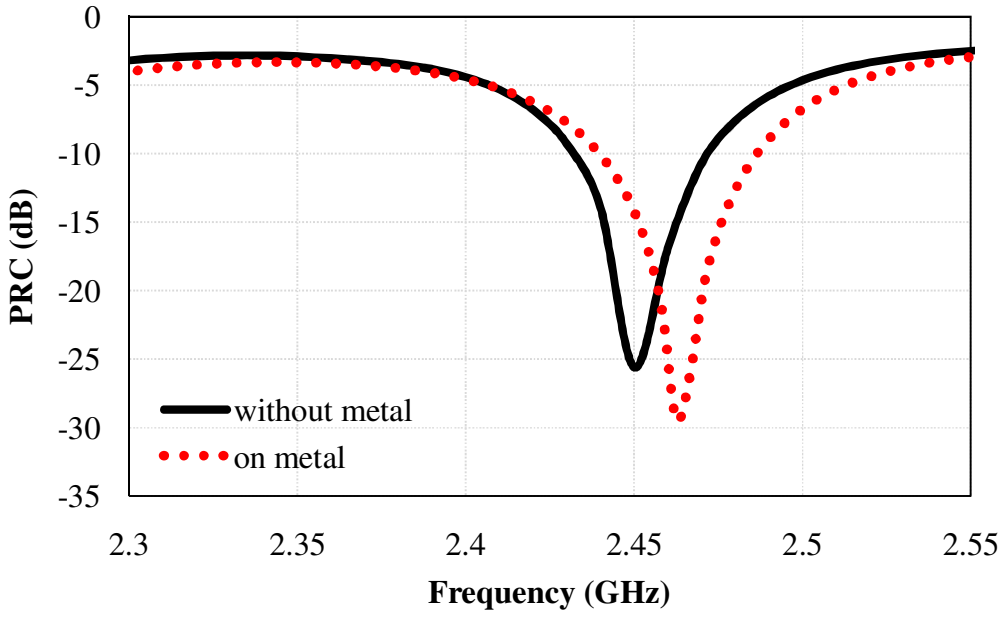

(a)

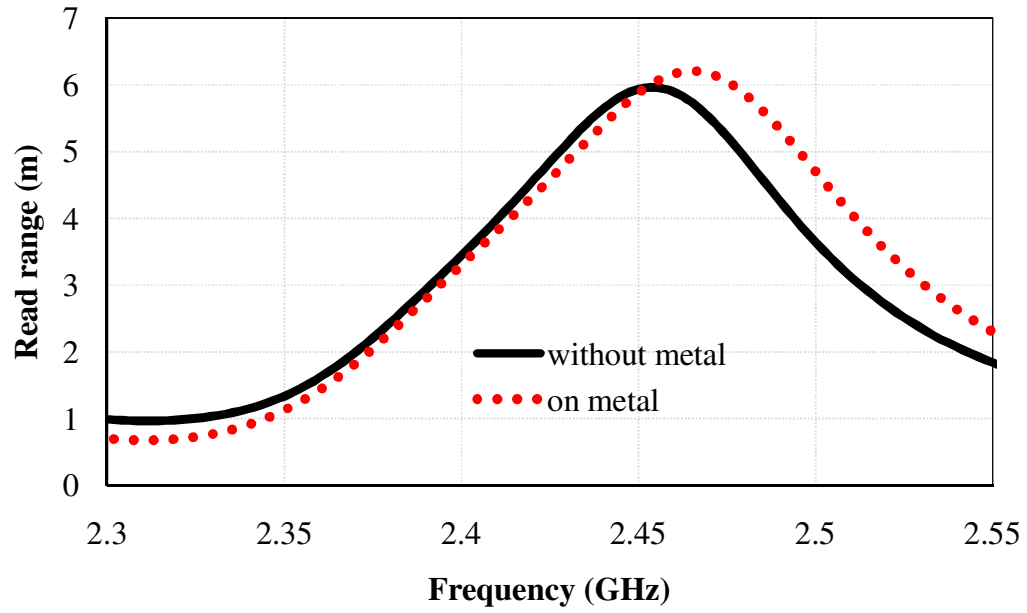

(b)

Figure 6.28: Simulated (a) power reflection coefficient and (b) read range of antenna in 2450 MHz

6.4. Summary

A dual-band single sided RFID Tag antenna operating in the UHF and SHF bands is presented that can be utilized for any kind of surfaces including metals. The proposed antenna utilized dual antenna structure for UHF band and conventional single antenna for SHF band. Use of dual-antenna at 915 MHz increases the differential RCS which results in enhancement of the read range. Maximum read range of the proposed antenna is found 5m at 915 MHz and 6m at 2450 MHz. The measured and simulated results are in agreement with respect to the input impedance of the antenna at 915 MHz and 2450 MHz.